Volume 7 | Issue 1 | June 2017 ISSN 2182-0287

Journal of Integrated OMICS

a methodological journal

JIOMICS

Journal of Integrated OMICS

Focus and Scope

Journal of Integrated OMICS, JIOMICS, provides a forum for the publication of original research papers, preliminary communications, technical notes and critical reviews in all branches of pure and applied "-omics", such as genomics, proteomics, lipidomics, metabolomics or metallomics. The manuscripts must address methodological development. Contributions are evaluated based on established guidelines, including the fundamental nature of the study, scientific novelty, and substantial improvement or advantage over existing technology or method. Original research papers on fundamental studies, and novel sensor and instrumentation development, are especially encouraged. It is expected that improvements will also be demonstrated within the context of (or with regard to) a specific biological question; ability to promote the analysis of molecular mechanisms is of particular interest. Novel or improved applications in areas such as clinical, medicinal and biological chemistry, environmental analysis, pharmacology and materials science and engineering are welcome.

North America

Randen Patterson
Center for Computational Proteomics, The Pennsylvania State University, USA

Oscar Alzate
Associate Professor of Cell and Developmental Biology, Adjunct Associate Professor in Neurology, Director: Systems Proteomics Center
School of Medicine, The University of North Carolina at Chapel Hill, USA

Yue Ge
US Environmental Protection Agency, Research Triangle Park, USA

South America

Eduardo Alves de Almeida
Depto. de Química e Ciências Ambientais, IBILCE - UNESP, Brazil

Marco Aurélio Zezzi Arruda
University of Campinas - Unicamp

Carlos H. I. Ramos
ChemistryInstitute – UNICAMP, Brazil

Associated editors

Africa

Saffaj Taouqif
Centre Universitaire Régional d'Interface, Université Sidi Mohamed Ben Abdallah, route d'Imouzzar-Fès, Morocco

Asia

Abdul Jaleel A
Rajiv Gandhi Centre for Biotechnology, Thycaud PO, Trivandrum, Kerala, India
Ali A. Ensafi
Isfahan University of Technology, Iran
Allison Stelling
Dresden, Germany
Amita Pal
Division of Plant Biology, Bose Institute, Kolkata, India
Ashish Gupta
Centre of Biomedical Magnetic Resonance, SGPGIMS Campus, Lucknow, India
Canhua Huang
The State Key Laboratory of Biotherapy, West China Hospital, Sichuan University, PR China
Chaminda Jayampath Seneviratne
Oral Biosciences, Faculty of Dentistry, University of Hong Kong, Hong Kong
Cheolju Lee
Korea Institute of Science and Technology, Seoul,Korea
Chi Chiu Wang
Department of Obstetrics & Gynaecology, Chinese University of Hong Kong, Hong Kong
Chii-Shiarng Chen
National Museum of Marine Biology and Aquarium, Checheng, Pingtung, Taiwan
Ching-Yu Lin
Institute of Environmental Health, College of Public Health, National Taiwan University, Taipei, Taiwan
Chantragan Srisomsap
Chulabhorn Research Institute, Bangkok, Thailand
Chen Han-Min
Department of Life Science, Catholic Fu-Jen University, Taipei, Taiwan
David Yew
Chinese University of Hong Kong, Shatin, N.T., Hong Kong
Debmalya Barh
Institute of Integrative Omics and Applied Biotechnology (IIOAB), India
Dwaipayan Bharadwaj
Genomics & Molecular Medicine Unit, Institute of Genomics & Integrative Biology (CSIR), Mall Road, Delhi, India
Eiji Kinoshita
Department of Functional Molecular Science, Graduate School of Biomedical Sciences, Hiroshima University, Japan
Eun Joo Song
Molecular Recognition Research Center, Korea Institute of Science & Technology, Seoul, Korea
Fan Chen
Institute of Genetics and Developmental Biology, Chinese Academy of Sciences (CAS), China
Feng Ge
Institute of Hydrobiology, Chinese Academy of Sciences, China
Ganesh Chandra Sahoo
BioMedical Informatics Center of Rajendra Memorial Research Institute of Medical Science (RMRIMS), Patna, India
Guangchuang Yu
Institute of Life & Health Engineering, Jinan University, Guangzhou, China
Gufeng Wang
Department of Chemistry, North Carolina State University, Raleigh, USA
Hai-Lei Zheng
School of Life Sciences, Xiamen University, China
Heebal Kim
Department of Food and Animal Biotechnology of the Seoul National University, Korea
Hsin-Yi Wu
Institute of Chemistry, Academia Sinica, Taiwan
Hitoshi Iwahashi
Health Research Institute, National Institute of Advanced Industrial Science

Australia and New Zealand

Mawson Institute, University of South Australia, Mawson Lakes, Australia
Michelle Hill
University of Queensland, Australia
Michelle Colgrave
CSIRO Livestock Industries, St Lucia, Australia
Nicolas Taylor
ARC Centre of Excellence in Plant Energy Biology & Centre for Comparative Analysis of Biomolecular Networks (CABiN), University of Western Australia, Perth, Australia
Peter Hoffmann
Institute for Photonics & Advanced Sensing (IPAS), School of Chemistry and Physics, University of Adelaide, Australia
Stefan Clerens
Protein Quality &Function, AgResearch Ltd Christchurch, New Zealand
Peter Solomon
Research School of Biology College of Medicine, Biology and Environment, Australian National University, Australia
Phoebe Chen
Department of Computer Science and Computer Engineering, La Trobe University, Melbourne, Australia
Richard Christopherson
School of Molecular Bioscience, University of Sydney, Australia
Sham Nair
Department of Biological Sciences, Faculty of Science, Macquarie University, NSW, Australia
Sylvia Urban
School of Applied Sciences (Discipline of Applied Chemistry), RMIT University, Melbourne, Victoria, Australia
Valerie Wasinger
Bioanalytical Mass Spectrometry Facility, Mark Wainwright Analytical Centre, University of NSW, Australia
Wujun Ma
Centre for Comparative Genomics, Murdoch University, Australia
Yin Xiao
Institute of Health and Biomedical Innovation, Queensland University of Technology, Australia

EUROPE

AhmetKoc, PhD
Izmir Institute of Technology, Department of Molecular Biology & Genetics, Urla, İzmir, Turkey
Alejandro Gella
Department of Basic Sciences, Neuroscience Laboratory, Faculty of Medicine and Health Sciences, Universitat Internacional de Catalunya,
Sant Cugat del Vallès-08195, Barcelona, Spain
Alessandro Pessione
Università degli Studi di Torino, Italy
Alexander Scherl
Proteomics Core Facility, Faculty of Medicine, University of Geneva, Geneva, Switzerland
Alfio Ferlito
ENT Clinic, University of Udine, Italy
Almudena Fernández Briera
Dpt. Biochemistry Genetics and Immunology, Faculty of Biology –University of Vigo, Spain
Alfonsina D'Amato
Politecnico di Milano, Department of Chemistry, Materials and Chemical Engineering "GiulioNatta", Italy
Alfred Vertegaal
Molecular Cell Biology, Leiden University Medical Center, The Netherlands
Ali Mobasheri
School of Veterinary Medicine and Science, Faculty of Medicine and Health Sciences, University of Nottingham, Sutton Bonington Campus, Sutton Bonington, Leicestershire, United Kingdom
Andre Almeida
Instituto de Tecnología Química e Biológica, Universidade Nova de Lisboa, Portugal
Andrea Matros
Leibniz Institute of Plant Genetics and Crop Plant Research (IPK-Gatersleben), Gatersleben, Germany
Andrei Turtoi
University of Liege, Metastasis Research Laboratory, GIGA-Cancer Bât. B23, Belgium
Angelo D'Alessandro
Università degli Studi della Tuscia, Department of Ecological and Biological Sciences, Viterbo, Italy
Angelo Izzo
Department of Experimental Pharmacology, University of Naples Federico II, Naples, Italy
Antonio Gnoni
Department of Medical Basic Sciences, University of Bari "Aldo Moro", Bari, Italy
Ana Maria Rodríguez-Piñeiro
Institute of Biomedicine, University of Gothenburg, Sweden
Ana Varela Coelho
Instituto de Tecnologia Química e Biológica (ITQB) Universidade Nova de Lisboa (UNL), Portugal
Anna Maria Timperio
Dipartimento Scienze Ambientali Università della Tuscia Viterbo, Italy
André Nogueira Da Costa
Molecular Carcinogenesis Group, Section of Mechanisms of Carcinogenesis International Agency for Research on Cancer - World Health Organization (IARC-WHO), Lyon, France
Andreas Boehm
Steigerfurtweg 8a, D-97084 Würzburg, Germany
Andrea Scaloni
Proteomics and Mass Spectrometry Laboratory, ISPAAM, National Research Council, via Argine 1085, 80147 Napoli, Italy
Andreas Tholey
Division for Systematic Proteome Research, Institute for Experimental Medicine, Christian-Albrechts-University, Germany
Angel Manteca
Departamento de Biologia Funcional and IUBA, Facultad de Medicina, Universidad de Oviedo, Spain
Angel P. Diz
Department of Biochemistry, Genetics and Immunology, Faculty of Biology, University of Vigo, Spain
Angela Bachi
Mass Spectrometry Unit DIBIT, San Raffaele Scientific Institute, Milano, Italy
Angela Chambery
Department of Life Science, Second University of Naples, Italy
Anna-Irini Koukkou
University of Ioannina, Department of Chemistry, Biochemistry Laboratory, Greece
António Sebastião Rodrigues
Departamento de Genética, Faculdade de Ciências Médicas, Universidade Nova de Lisboa,Portugal
Arkadiusz Kosmala
Laboratory of Cytogenetics and Molecular Biology, Institute of Plant Genetics, Polish Academy of Sciences, Poland

Center for Plant Molecular Biology, EberhardKarls University Tübingen, Tübingen, Germany

Valeria Bertagnolo
Department of Morphology and Embryology University of Ferrara, Italy

Vera Muccilli
DipartimentodiScienzeChimiche, UniversitàdiCatania, Catania, Italy

Veronica Mainini
Dept. Health Science, University of Milano-Bicocca, Faculty of Medicine, Monza (MB), Italy

Vicenta Martínez-Zorzano
Department of Biochemistry, Genetics and Immunology
University of Vigo, Spain

Virginie Brun
French Atomic Energy Commission and *French National Institute* for *Health* and Medical Research, France

Vittoria Matafora
Biological Mass Spectrometry Unit, San Raffaele Scientific Institute, Milan, Italy

Vladislav Khrustalev
Department of General Chemistry, Belarussian, State Medical University, Dzerzinskogo, Minsk, Belarus

Xiaozhe Zhang
Department of Medicine, University of Frioburg, Switzerland

Yuri van der Burgt
Leiden University Medical Center, Department of Parasitology, The Netherlands

SOUTH AMERICA

Alessandro Farias
Neuroimmunomodulation Group, department of Genetics, Evolution and Bioagents, University of Campinas - SP – Brazil

Alexandra Sawaya
Department of Plant Biology, Institute of Biology, UNICAMP, Campinas, São Paulo, Brazil

Andréa P.B. Gollucke
Hexalab/Catholic University of Santos, Brazil

Arlindo Moura
Department of Animal Science - College of Agricultural Sciences - Federal University of Ceara, Fortaleza, Brasil

Bruno Lomonte
Instituto Clodomiro Picado, Universidad de Costa Rica

Deborah Schechtman
Department of Biochemistry, Chemistry Institute, University of São Paulo, Brazil

Edson Guimarães Lo Turco
São Paulo Federal University, Brasil

Elisabeth Schwartz
Department of Physiological Sciences, Institute of Biological Sciences, University of Brasilia, Brazil

Fabio Ribeiro Cerqueira
Department of Informatics and NuBio (Research Group for Bioinformatics), University of Vicosa, Brazil

Fernando Barbosa
Faculty of Pharmaceutical Sciences of Ribeirão Preto University of São Paulo, Brazil

Hugo Eduardo Cerecetto
Grupo de Química Medicinal, Facultad de Química, Universidad de la República, Montevideo, Uruguay

Luis Pacheco
Institute of Health Sciences, Federal University of Bahia, Salvador, Brazil

Mário Hiroyuki Hirata
Laboratório de Biologia Molecular Aplicado ao Diagnóstico, Departamento de Análises Clínicas e Toxicológicas, Faculdade de Ciências Farmacêuticas, Universidade de São Paulo, Brazil

Jan Schripsema
Grupo Metabolômica, Laboratório de Ciências Quimicas, Universidade Estadual do Norte Fluminense, Campos dos Goytacazes, Brazil

Jorg Kobarg
Centro Nacional de Pesquisa em Energia e Materiais, Laboratório Nacional de Biociências, Brazil

Marcelo Bento Soares
Cancer Biology and Epigenomics Program, Children's Memorial Research Center, Professor of Pediatrics, Northwestern University's Feinberg School of Medicine

Mario Palma
Center of Study of Social Insects (CEIS)/Dept. Biology, Institute of Biosciences, Univesity of São Paulo State (UNESP), Rio Claro - SP Brazil

Rinaldo Wellerson Pereira
Programa de Pós Graduação em Ciências Genômicas e Biotecnologia, Universidade Católica de Brasília, Brazil

Roberto Bobadilla
BioSigma S.A., Santiago de Chile, Chile

Rossana Arroyo
Department of Infectomic and Molecular Biology, Center of Research and Advanced Studies of the National, Polytechnical Institute (CINVESTAV-IPN), Mexico City, Mexico

Rubem Menna Barreto
Laboratorio de Biología Celular, Instituto Oswaldo Cruz, Fundaçao Oswaldo Cruz, Rio de Janeiro, Brazil

Vasco Azevedo
BiologicalSciencesInstitute, Federal University of Minas Gerais, Brazil

NORTH AMERICA

Adam Vigil
University of California, Irvine, USA

Akeel Baig
Hoffmann-La Roche Limited, Pharma Research Toronto, Toronto, Ontario, Canada

Alexander Statnikov
Center for Health Informatics and Bioinformatics, New York University School of Medicine, New York

Amosy M'Koma
Vanderbilt University School of Medicine, Department of General Surgery, Colon and Rectal Surgery, Nashville, USA

Amrita Cheema
Georgetown Lombardi Comprehensive Cancer Center, USA

Anthony Gramolini
Department of Physiology, Faculty of Medicine, University of Toronto, Canada

Anas Abdel Rahman
Department of Chemistry, Memorial University of Newfoundland and Labrador St. John's, Canada

Christina Ferreira
Purdue University - Aston Laboratories of Mass Spectrometry, Hall for Discovery and Learning Research, West Lafayette, US

Christoph Borcher

JOURNAL OF INTEGRATED OMICS

A methodological Journal

CONTENTS OF VOLUME 7 | ISSUE 1 | JUNE 2017

ORIGINAL ARTICLES

SELECTED ABSTRACTS OF THE 5TH INTERNATIONAL CONGRESS ON ANALYTICAL PROTEOMICS (ICAP 2017)

JOURNAL OF INTEGRATED OMICS
A METHODOLOGICAL JOURNAL
HTTP://WWW.JIOMICS.COM

ORIGINAL ARTICLE | DOI: 10.5584/jiomics.v7i1.200

Comparative integrated omics approach sterically understanding hepatic metabolic dynamics in mouse model

Shoko Takahashi[1,2], Huijuan Jia[2], Kenji Saito[2] and Hisanori Kato[2]*

[1] Department of Applied Biological Chemistry, Graduate School of Agricultural and Life Sciences, The University of Tokyo, 1-1-1, Yayoi, Bunkyo-ku, Tokyo, Japan. [2] Food for Life, Organization for Interdisciplinary Research Projects, The University of Tokyo, 1-1-1, Yayoi, Bunkyo-ku, Tokyo, Japan.

Received: 20 September 2016 **Accepted:** 24 November 2016 **Available Online**: 18 January 2017

ABSTRACT

Currently, omics-fusion, which is the combined analysis of data by employing multiple omics analyses, has been available, and it can enable a more fundamental understanding of the biological phenomena than a single omics. However, multi-layered combination of multiple omics technologies involves generation of a large amount of data, which leads to increased complexity and makes comprehension of bio-information more difficult. The objective of this study was to investigate the utility of incorporating multiple omics technologies in a multi-layered fashion. Transcriptomic, proteomic, and metabolomic analyses were carried out using a mouse model of diet-induced obesity. The present study reported the comprehensiveness of three omics analyses and the utility of using multiple omics analyses. Some uniform changes among different omis were observed, but the majority of changes were specific to each omics approach. This data supports the fact that various molecules progress through the central dogma at differing speeds. Since the time axis differs for each molecule, combining multiple omics analyses makes it possible to investigate the reactions in organisms three-dimensionally. At first glance, it simply appears that combining a number of very large data sets produces even more complexity but, if multi-layered omics data are treated with an awareness of their meaning, benefits, and limitations, then the combination of multiple omics analyses can be extremely useful for research in molecular biology.

Keywords: transcriptomics, proteomics, metabolomics, multi-omics .

Abbreviations: CE-TOF MS (Capillary electrophoresis time-of-flight mass spectrometry), FDR (False discovery rate), HF (High-fat diet), TRAQ (Isobaric tags for relative and absolute quantitation), LC-TOF MS (Liquid chromatography time-of-flight mass spectrometry), ND (Normal diet), PPARg (peroxisome proliferator-activated receptor gamma), RMA (Robust Multi-array Average).

1. Introduction

The Genome Project revealed the genomic sequences a variety of living organisms, including humans, and this information has fueled research into the comprehensive understanding of genomes. Appending the suffix 'omics' to the subject of study gives rise to the specific research area, such as genomics, transcriptomics, proteomics, and metabolomics. Such omics studies can aid the understanding of the influence of drug or food on homeostasis or the metabolic system, their role in disease prevention, and the relationship between the individual's genotype and disease [1-3]. As this type of omics approach is utilized in various research tasks, such as evaluating the functionality of drug or food, clarifying its mechanisms of action, and predicting toxicity, it can be proposed that with the spread of omics technologies, demand for such research will increase in the fields of lifescience research. Currently, omics-fusion, which is the combined analysis of data by employing multiple omics analyses, has been available, and it can enable a more fundamental understanding of the biological phenomena than a single omics. Most recently, omics analysis tool PGMiner has been published [4]. Furthermore, some integrated omics studies have been reported, for example, integration of protein, mRNA and miRNA [5], transcriptome and metagenome [6], transcriptome and proteome [7-9].

***Corresponding author:** Hisanori Kato, The University of Tokyo, 1-1-1 Yayoi, Bunkyo-ku, Tokyo 113-8657, Japan. Phone number: +81 358411607. Email Address: akatoq@mail.ecc.u-tokyo.ac.jp

However, multi-layered combination of multiple omics technologies involves generation of a large amount of data, which leads to increased complexity and makes comprehension of bio-information more difficult. The objective of this study was to investigate the utility of incorporating multiple omics technologies in a multi-layered fashion. Our group has been doing various research about the prevention of lifestyle diseases including diabetes and metabolic disorder [10]. The utility of multiple omics technologies may be a powerful tool for the research region about the prevention of lifestyle diseases like obesity and metabolic syndrome, in the field of nutriomics like this study, when the lifestyle choices are properly correlated. Therefore, transcriptomic, proteomic, and metabolomic analyses were carried out using a mouse model of diet-induced obesity, which is one of the most commonly utilized models in obesity research. Additionally, a verification experiment on multi-layered omics was performed by comparison and investigation of these data.

2. Material and Method

2.1. Animal experiments

Male C57BL/6J mice purchased from Charles River Laboratories Japan, Inc., at 7 weeks of age were divided into two groups, the normal diet group (ND group) was fed D12450B (10 kcal% fat, Research Diets) and the high-fat diet group (HF group) was fed D12492 (60 kcal% fat, Research Diets). They were housed individually at a controlled temperature of 23±1°C under a 12-h light-12-h dark cycle. After fed ad libitum for 9 weeks, on the last day of the experiment, after a 16-h food deprivation and a 1.5-h re-feeding, the mice were deeply anesthetized with an intraperitoneal injection of sodium pentobarbital. The livers were then excised and proceeded to each omics analysis. The same samples were analyzed in transcriptomics, proteomics, and metabolomics studies (n=3 for each group). All animal experiments were carried out in accordance with the guidelines of the Animal Usage Committee of the Faculty of Agriculture of the University of Tokyo.

2.2. Transcriptomics using DNA microarray data

DNA microarray data used in the present study were obtained in the previous experiment, which were carried out with Affymetrix GeneChip Mouse Genome 430 2.0 array (Affymetrix, Santa Clara, CA, USA), which has 45,000 probe sets and can analyze the expression level of over 39,000 transcripts and variants from over 34,000 well characterized mouse genes [10]. Briefly, total RNA was isolated from the livers of these mice using TRIzol Reagent (Invitrogen Life Technologies, Tokyo, Japan). RNA of each individual was reverse-transcribed to the first-strand complementary DNA using SuperScript II RT (Invitrogen Life Technologies, Tokyo, Japan). Second-strand complementary DNA synthesis was then carried out using a DNA polymerase. Biotinylated complementary RNA was generated from the complementary DNA using a BioArray HighYield RNA transcript labeling kit (Enzo Life Sciences, Farmingdale, NY, USA) according to the standard Affymetrix protocols. The obtained intensity files were analyzed using the statistical analysis software R. After normalization of the intensity files was performed with robust multi-array average (RMA) normalizing [11], and then a clustering analysis was done with hclust (hierarchical clustering, average linkage). Rank products was used for intergroup comparison [12]. The expression change was taken as informative when the false discovery rate (FDR) value was < 0.1. To obtain detailed molecular information and infer significant signaling pathways from global profiling results of DNA microarray data, we uploaded differentially expressed gene probes according to the above criteria to DAVID (The Database for Annotation, Visualization and Integrated Discovery, https://david.ncifcrf.gov/).

2.3. Proteomics

We performed the differential proteomic analysis of the mouse livers using Isobaric tags for relative and absolute quantitation (iTRAQ), the same methods as our previous study [13]. iTRAQ are a non-gel-based technique used to quantify proteins from different sources in a single experiment. It uses isotope-coded covalent tags. Total protein was extracted by using lysis buffer and separated by centrifugation at 12,000 × g for 30 min at 4 °C. Protein concentrations were determined using the Bradford assay, and pooled protein were proceed to iTRAQ experiment kit, performed according to the manufacture's protocol (AB SCIEX). Desalted samples were vacuum evaporated, and added 50 µl of 0.1% formic acid, and 2 µl of samples were measured with LC/MS/MS (TripleTOFTM 5600 + System with Eksigent nanoLC). ProteinPilot™ (AB SCIEX) was used to identify proteins and calculate protein expression levels by comparing *in silico* peptide data. The number of peptides used to identify proteins were shown in Table 2.

2.4. Metabolomics

Frozen mice liver samples were transferred into 500 µL of methanol containing 50 µM of external standard. After homogenization by BMS-M10N21 (bms, Tokyo) at 1,500 rpm, 120 s five times, 500 µL of chloroform and 200 µL of ultra-pure water were added to the homogenate and mixed well and centrifuged at 2,300 g for 5 min at 4°C. The resultant water phases were ultrafiltrated by the Millipore Ultrafree-MC PLHCC HMT Centrifugal Filter Device, 5 kDa (Millipore, Billerica, MA). The filtrates were dried and dissolved in 50 µL of ultra-pure water. We then subjected the samples obtained to capillary electrophoresis time-of-flight mass spectrometry (CE-TOFMS) analysis using the Agilent CE-TOFMS system (Agilent Technologies, Santa Clara, CA)

Table 1. GO enriched terms of differentially expressed genes

Increased	*p*-value	Decreased	*p*-value
Steroid biosynthesis	7.10E-21	Phosphoprotein	1.80E-09
Sterol biosynthetic process	4.20E-20	Cell fraction	3.50E-07
Steroid metabolic process	5.40E-20	Insoluble fraction	3.90E-06
Sterol biosynthesis	3.50E-19	Cytoplasm	5.20E-06
Steroid biosynthetic process	1.50E-18	Membrane fraction	2.10E-05
Cholesterol biosynthetic process	2.20E-17	Endoplasmic reticulum	3.60E-05
Sterol metabolic process	1.70E-16	Ubl conjugation	9.00E-05
Cholesterol biosynthesis	4.30E-16	Stress response	1.00E-04
Cholesterol metabolic process	8.20E-14	PPAR signaling pathway	1.90E-04
Lipid synthesis	1.50E-13	Endoplasmic reticulum	2.20E-04
Lipid biosynthetic process	1.40E-12	Microsome	2.20E-04
Oxidoreductase	1.60E-12	Membrane	2.40E-04
Endoplasmic reticulum	2.60E-12	Golgi apparatus	2.60E-04
Steroid biosynthesis	4.50E-12	Vesicular fraction	3.00E-04
Oxidation reduction	5.30E-12	Lipoprotein	4.60E-04
Endoplasmic reticulum	1.40E-10	Acetylation	5.00E-04
Terpenoid backbone biosynthesis	4.00E-08	Steroid metabolic process	5.60E-04
Transferase activity, transferring alkyl or aryl (other than methyl) groups	8.90E-08	Regulation of hydrolase activity	7.00E-04
Microsome	1.80E-07	Basolateral plasma membrane	7.10E-04
Cell fraction	2.00E-07	Cytosol	1.20E-03
Vesicular fraction	2.90E-07	Golgi apparatus	1.20E-03
Isoprenoid metabolic process	3.20E-07	Steroid dehydrogenase activity	1.50E-03
Isoprenoid biosynthetic process	7.70E-07	Nucleotide binding	2.00E-03
Insoluble fraction	9.20E-07	Small GTPase mediated signal transduction	2.10E-03
Membrane fraction	1.30E-06	Trophectodermal cell differentiation	2.50E-03
Binding site:Substrate	3.10E-06	Histone H3	2.60E-03
Peroxisome	5.90E-06	H3	2.70E-03
Microbody	5.90E-06	NADP	2.90E-03
Acetylation	1.40E-05	Leukocyte transendothelial migration	3.00E-03
Peroxisome	1.70E-05	Extrinsic to membrane	3.10E-03

*P-value is Fisher's exact test

Table 2. The list of increased or decreased proteins by high-fat diet.

Protein	Name	Protein ID	# of Peptides	Fold Change	p-value
AL1A1	Retinal dehydrogenase 1	P24549	66	2.001	0.000
CAH3	Carbonic anhydrase 3	P16015	71	1.969	0.000
BHMT1	Betaine--homocysteine S-methyltransferase 1	O35490	76	1.907	0.000
HBB1	Hemoglobin subunit beta-1	P02088	79	1.879	0.018
THIL	Acetyl-CoA acetyltransferase, mitochondrial	Q8QZT1	44	1.548	0.000
AL3A2	Fatty aldehyde dehydrogenase	P47740	17	1.538	0.003
RLA2	60S acidic ribosomal protein P2	P99027	35	1.524	0.022
OAT	Ornithine aminotransferase, mitochondrial	P29758	27	1.518	0.039
RL7A	60S ribosomal protein L7a	P12970	5	1.506	0.066
PRDX6	Peroxiredoxin-6	O08709	51	1.489	0.003
NLTP	Non-specific lipid-transfer protein	P32020	70	1.475	0.001
PDIA1	Protein disulfide-isomerase	P09103	57	1.468	0.001
RL23A	60S ribosomal protein L23a	P62751	9	1.448	0.035
HCD2	3-hydroxyacyl-CoA dehydrogenase type-2	O08756	17	1.403	0.078
GSTA3	Glutathione S-transferase A3	P30115	22	1.400	0.084
APOA1	Apolipoprotein A-I	Q00623	20	1.380	0.001
GGLO	L-gulonolactone oxidase	P58710	7	1.378	0.003
PHS	Pterin-4-alpha-carbinolamine dehydra-	P61458	13	1.373	0.067
EF1A1	Elongation factor 1-alpha 1	P10126	39	1.369	0.015
DHB5	Estradiol 17 beta-dehydrogenase 5	P70694	31	1.367	0.051
DHSO	Sorbitol dehydrogenase	Q64442	45	1.359	0.003
AATM	Aspartate aminotransferase, mitochondrial	P05202	45	1.356	0.000
DECR	2,4-dienoyl-CoA reductase, mitochondrial	Q9CQ62	21	1.331	0.029
TTC36	Tetratricopeptide repeat protein 36	Q8VBW8	18	1.329	0.044
TALDO	Transaldolase	Q93092	8	1.315	0.083
GLNA	Glutamine synthetase	P15105	30	1.313	0.011
FAAA	Fumarylacetoacetase	P35505	44	1.286	0.004
CK054	Ester hydrolase C11orf54 homolog	Q91V76	10	1.275	0.054
CALR	Calreticulin	P14211	28	1.273	0.046
PDIA3	Protein disulfide-isomerase A3	P27773	50	1.263	0.042
MAOX	NADP-dependent malic enzyme	P06801	13	0.357	0.084
FAS	Fatty acid synthase	P19096	75	0.475	0.000
ACLY	ATP-citrate synthase	Q91V92	24	0.517	0.000
KPYR	Pyruvate kinase isozymes R/L	P53657	30	0.581	0.001
ACOT1	Acyl-coenzyme A thioesterase 1	O55137	4	0.589	0.014
ECHP	Peroxisomal bifunctional enzyme	Q9DBM2	49	0.610	0.000
OPLA	5-oxoprolinase	Q8K010	3	0.618	0.070
GSTP1	Glutathione S-transferase P 1	P19157	69	0.662	0.024
GPDM	Glycerol-3-phosphate dehydrogenase, mitochondrial	Q64521	8	0.686	0.014
RS13	40S ribosomal protein S13	P62301	6	0.701	0.025
APOA4	Apolipoprotein A-IV	P06728	6	0.711	0.078
ODP2	Dihydrolipoyllysine-residue acetyltransferase component of pyruvate dehydrogenase complex, mitochondrial	Q8BMF4	9	0.717	0.098
CY1	Cytochrome c1, heme protein, mitochondrial	Q9D0M3	17	0.741	0.070
PCCB	Propionyl-CoA carboxylase beta chain, mitochondrial	Q99MN9	14	0.747	0.092
DHAK	Bifunctional ATP-dependent dihydroxyacetone kinase/ FAD -AMP lyase (cyclizing)	Q8VC30	35	0.805	0.062
GLCTK	Glycerate kinase	Q8QZY2	4	0.812	0.061
PBLD2	Phenazine biosynthesis-like domain-containing protein 2	Q9CXN7	16	0.818	0.098
ALDOB	Fructose-bisphosphate aldolase B	Q91Y97	77	0.821	0.035
ANXA6	Annexin A6	P14824	14	0.839	0.086
GLGB	1,4-alpha-glucan-branching enzyme	Q9D6Y9	11	0.839	0.057
DPYD	Dihydropyrimidine dehydrogenase [NADP+]	Q8CHR6	7	0.843	0.087
PYC	Pyruvate carboxylase, mitochondrial	Q05920	73	0.870	0.041
CPSM	Carbamoyl-phosphate synthase [ammonia], mitochon-	Q8C196	360	0.872	0.004

at 4°C. The alignment of detected peaks was performed according to the m/z value and normalized migration time. The relative area value of each peak was calculated and used for the intergroup comparison. Samples that were obviously characterizing outliers were eliminated from the analysis. Metabolite extraction, MS analysis, and data analysis were performed in Human Metabolome Technologies.

2.5. Integrated analysis of transcriptomics and metabolomics

We used the web-based tool Keggle (http://keggle.jp), a novel tool for the visualization of omics-data created by the author's group [14]. Transcriptome and metabolome data were mapped onto KEGG (Kyoto Encyclopedia of Genes and Genomes, http://www.genome.jp/kegg/) pathways on the web.

3. Results

3.1. Animal experiments

The final body weights were higher in the HF group compared to the ND group. The C57BL/6J mouse used in this study is regarded as relatively sensitive to high-fat diets and suitable as a non-genetic obese animal model when fed a high-fat diet. The body weight gain of the mice fed a high-fat diet (60% energy) for 9 weeks was 17.2 g, whereas that of the mice fed a normal diet was 4.59 g, suggesting that the mice fed a high-fat diet in this study can be regarded as a valid obesity model for research (Supplemental Figure S1).

3.2. Results of DNA microarray data

Among the total 817 differentially expressed gene probes, 480 gene probes showed increases, and 337 gene probes showed decreases in HF group. These differentially expressed genes were uploaded to DAVID functional annotation tools and the enrichment analysis was performed (Table 1). The top 10 of enriched terms of increased genes were Steroid biosynthesis, Sterol biosynthetic process, Steroid metabolic process, Sterol biosynthesis, Steroid biosynthetic process, Cholesterol biosynthetic process, Sterol metabolic process, Cholesterol biosynthesis, Cholesterol metabolic process, Lipid synthesis, lipid biosynthetic process.

3.3. Results of proteome analysis using iTRAQ method

The proteome of mouse liver were analyzed using iTRAQ labeling and LC/MS/MS. Among identified 1043 proteins, 50, 23 proteins were significantly increased and decreased by HF, respectively (p-value < 0.1). In these proteins which showed changes, the most differentially expressed proteins were shown in Table 2. Among the increased proteins, ALDH1A1, HSD17B10, APOA1, AKR1C4, GOT2 and ACSL1 are related to the oxidation of fat. Furthermore, lipid transport proteins, including SCP2, APOA1, GOT2 and ACSL1, and oxidative stress proteins including PRDX2 and PRDX6 were increased. In the decreased proteins, there were APOA4, ACLY, FASN and DECR1, which related to fatty acid synthesis, PKLR and PCX, which related to glucose metabolism, ME1 and ACLY, which related to TCA cycle. These alterations mean that lipid oxidation, transport and oxidative stress were increased and TCA cycle, fatty acid synthesis and glucose metabolism were decreased in the liver tissue of obese mouse.

3.4. Results of metabolome analysis

We performed a metabolome analysis to explore the hepatic metabolic alterations underlying the effects of HF diet. Among the peaks obtained from the CE- and LC-TOF MS analysis, 385 peaks were identified according to the value of m/z and MT from metabolite database. Of these metabolites, 26 showed changes, 10 were increased and 16 were decreased (Table 3). N-acetylglutamate (N-AcGlu), which is a positive regulator of the urea cycle, was decreased by the high-fat diet. Similar changes were found in the abundance of ornithine, citruline, argininosuccinate (ArgSuccinate), and arginine, which are the intermediates of the urea cycle, and the final product, urea. In diet-indused obese animal, it is well known that the urea production is decreased by the dysfunction of urea cycle related enzymes [15].

Furthermore, the abundance of choline was decreased by HF diet. Choline is known to be a nutrient, which prevent the accumulation of hepatic triglyceride, and reported to be decreased in hepatosteatosis mouse liver [16].

4. Discussion

It is widely accepted amongst molecular biologists that analysis based on these omics analyses is extremely effective, and rapid technological innovation such as high-throughput DNA sequencing and high-precision electron impact mass spectrometry as well as improvements in DNA microarray chips have led to its frequent utilization in various fields. Prior to the popularization of omics technology, research was carried out by focusing on a target molecule from a wider range of biomolecules, but the utilization of omics has led to a significant increase in the number of molecules that can be captured. Omics analysis is not a tool for arriving at conclusions, but is rather an approach for unbiased screening. Even though currently DNA microarray probably would've been easier to analyze data through many analysis tools, using RNA-seq technology would become less biased. Furthermore, taking into account the complexity of the interactions between food, pharmaceuticals, and the organism, methods that provide a complete overview of the influences on the biomolecules should lead to rapid research progress. However, while the use of omics technology has

Table 3. The list of increased or decreased metabolites by high-fat diet

KEGG ID	Compound name	Fold change	p-value
No ID	1H-Imidazole-4-propionic acid	3.693	0.006
C00167	UDP-glucuronic acid	2.565	0.018
C00149,C00497, C00711	Malic acid	2.048	0.029
C00122	Fumaric acid	2.014	0.037
C01879	5-Oxoproline	1.863	0.010
No ID	Heptadecanoic acid	1.649	0.037
C00307	CDP-choline	1.503	0.032
C00262	Hypoxanthine	1.503	0.034
No ID	Stearoyl ethanolamide	1.435	0.016
C01081	Thiamine phosphate	1.376	0.017
No ID	2-Hydroxyisobutyric acid	0.852	0.014
C00780	Serotonin	0.831	0.010
C00086	Urea	0.786	0.022
C00114	Choline	0.753	0.032
No ID	Homoserinelactone	0.669	0.014
C03425	Methyl oleate	0.643	0.029
C00042	Succinic acid	0.641	0.049
C00601	Phenylacetaldehyde	0.632	0.036
C01026	N,N-Dimethylglycine	0.569	0.029
C05568	Imidazolelactic acid	0.465	0.007
C03406	Argininosuccinic acid	0.440	0.007
C02835	Imidazole-4-acetic acid	0.424	0.042
No ID	AC(22:0)	0.412	0.008
C02592	Taurolithocholic acid	0.321	0.030
C00489	Glutaric acid	0.273	0.015
C01921	Glycocholic acid	0.241	0.035

spread to molecular biology and numerous studies utilizing omics technology have been conducted, this technology was not employed effectively in a large number of studies. Therefore, it is important to have a clear understanding of the problems that omics can solve.

Fundamentally, when the research objective or task (the 'why') is clear, the four aspects of 'where', 'when', 'what', and 'how' on which the analysis will be carried out are of importance. For example, in an experiment conducted in this study, these aspects are—what will be fed and on which organ or cell the changes will be observed (where), when will the analysis take place in the experiment schedule (when), which molecule is observed in the selected cell or time (what), and how the data will be analyzed (how). If, the research design is broken down into these four aspects, the factor that omics can solve is the 'what' factor, i.e., a large number of biomolecules can be captured at once. In molecular biology research, omics technology does not solve the 'where' or 'when', overwhelmingly solves the 'what', and makes solving the 'how' more difficult. Employing multiple omics in a multi-layered fashion will broaden the field of observation for the 'what' and make the 'how' more difficult due to increased complexity. Because a large amount of data on biomolecules can be gathered, knowledge about bioinformatics becomes necessary and a situation arises where the acquired data is so vast that it becomes difficult to analyze. The discernment of false-negatives and false-positives also becomes a problem. Even though a variety of tools for performing omics analysis have become prevalent, and tools such as the Ingenuity pathway analysis (IPA, http://www.ingenuity.com), KeyPathwayMiner (http://tomcat.compbio.sdu.dk/keypathwayminer/) [17, 18] and DAVID are used in most research labs, the problem of 'how' still remains a challenge for the future. Despite the presence of these kinds of benefits and challenges, when the complexity of the central dogma is taken into consideration, it can be proposed that there would be large benefits from employing omics in a multi-layered fashion at multiple levels such as mRNA, protein, and metabolite.

In this experiment, omics analysis was performed at three levels—gene expression, protein expression, and metabolite formation. When considering the comprehensiveness of these omics approaches, it is first necessary to consider that the number and characteristics of the molecules, which are the targets of these omics, are all different. Figure 1 represents the molecule count for the subject of analysis and the number of molecules that were detectable in this experiment for the three stages (molecule count is presented as logarithm). The number of genes in the mouse used in this animal experiment is said to be approximately 30,000 [19], with over 20,000 being detectable using DNA microarray. DNA micro array is said to have a higher comprehensiveness than other omics, but the reason for this is that the molecules of interest all have the same properties. Additionally, it is said that there are between 500,000 to 1 million types of proteins, with approximately 1,000 being able to be detected by proteomics in this experiment (Figure 1)—the lowest comprehensiveness as compared to

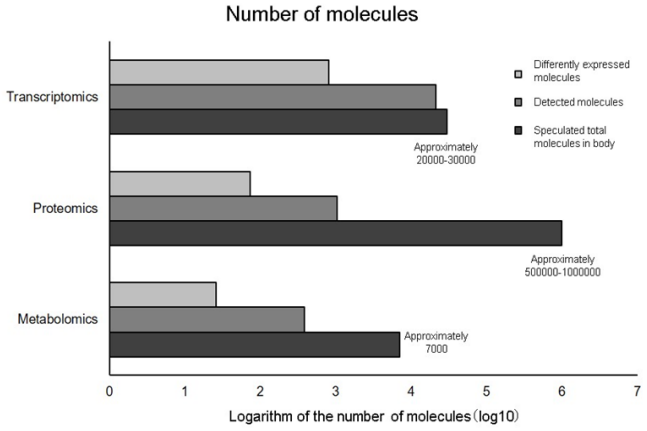

Figure 1. The comprehensiveness of each omics technique.
Molecule count for the subject of analysis and the number of molecules that were detectable in this experiment for the three stages are represented (molecule count is presented as logarithm).

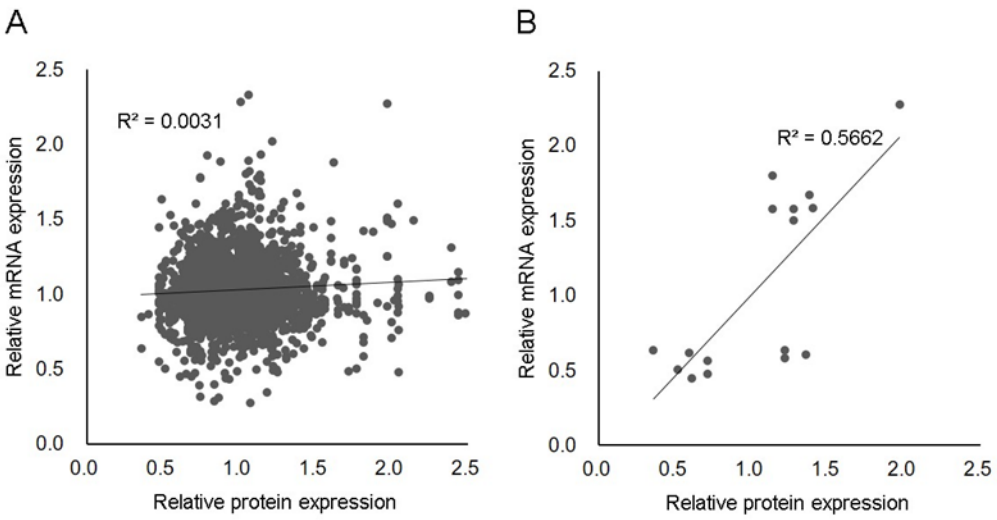

Figure 2. A correlation plot of the change in scaling factors of the transcriptomics and proteomics data.
(A) The plot of the whole data, **(B)** Extracting and plotting the significant changes in the transcriptomics and proteomics data.

transcriptomics. The reason for this is that physical properties of each protein differ, and from a technical point of view, a method with high comprehensiveness has not yet been established. Furthermore, according to a study by Wishart et al. (2007) [20], approximately 7,000 molecules (approximately 2500 metabolites, 1200 pharmaceuticals, and 3500 food based elements) existed as target metabolite molecules in metabolomics. As the physical properties of metabolites differ by each molecule, there is no one technique, which can comprehend everything at the same time. In this experiment, metabolomics was carried out through the combination of CE-TOF/MS and LC-TOF/MS, resulting in the successful detection of 385 metabolites (Figure 1). Comparing the comprehensiveness of the three omics analyses, we noted that proteomics has the lowest comprehensiveness. However, there are striking innovations in current proteome analysis technology including the iTRAQ method employed in this study, which is a shotgun method in proteomics that uses stable radioactive isotopes. Currently, differences in comprehensiveness do exist but they will be resolved over time as technology improves.

When conducting research involving multiple omics, it is necessary to be aware that the molecule counts will differ and for technological reason, large differences in comprehensiveness will exist between various omics analyses. Specifically, attention should be given to the method of applying multiple omics data. It is essential to understand that there is a reason for the common change that exists in the multiple omics data and to approach the issue from this point. As noted above, the reason for this is that there are large differences in the comprehensiveness between omics; to have a common difference means to be tied to the weakness of the statistical power of the omics approach with the lowest comprehensiveness. The next section discusses the presence of uniform changes for different omics approaches at different stages when dealing with multiple omics data.

This study compared the transcriptomics and proteomics data in order to consider the uniformity between results of different omics. First, a correlation plot of the change in scaling factors of the transcriptomics and proteomics data was created (Figure 2). The plot of the whole data does not show any particular correlation (Figure 2-A). Extracting and plotting the significant changes in the transcriptomics and proteomics data reveals a high level of correlation (Figure 2-B). Molecules exhibiting changes in the same direction (increase/decrease in expression) were extracted from the data and those exhibiting common changes for both transcriptomics and proteomics, were listed in Supplemental Table S1. There were eleven molecules where a common change was noted in the mRNA and protein levels, summing up to 15.1% of the number of changes in protein count observed through proteomics.

As is the case for the molecules in Supplemental Table S1, a number of things can be said about the fact that a common change can be observed among multiple stages. Because they possess a quality, which makes it possible to observe the same change at multiple stages at the exact moment the analysis occurs, it can be said that there is no need to conduct analyses at multiple stages for molecules with the same observed change. However, in fact, the same change can be observed which will increase the reliability of the data. The fact that the changes in the mRNA level can also be observed in the protein level (which catalyzes the actual response in the organism) makes it easier to understand the meaning of the mRNA change. Further, the change in mRNA also provides support as to why the change in protein level occurs. Obtaining a single change from

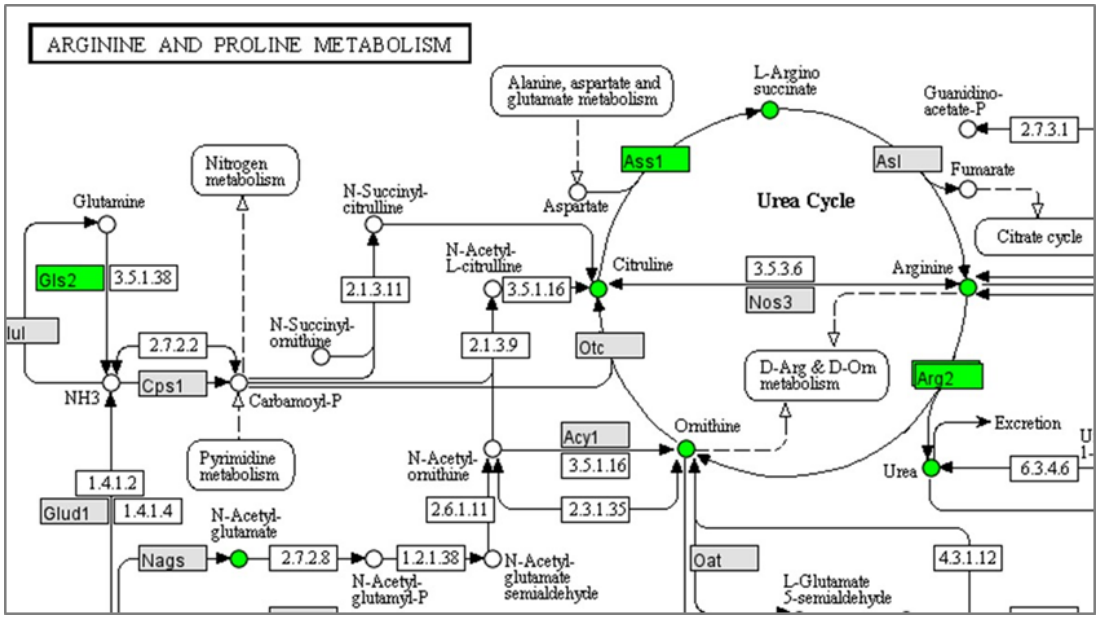

Figure 3. The metabolic and transcriptomic change in the urea cycle.
The metabolic and transcriptomic change in the urea cycle were represented by mapping simultaneously on a KEGG metabolism map using Keggle analysis tool. Decreased expression of transcripts or metabolites showed green color.

multiple stages enables observation from a three-dimensional perspective. One needs to be aware of the above point regarding the comprehensiveness when considering uniformity. While it is true that uniformity in multiple omics data leads to higher reliability, this will not mean that high reliability of data will lead to uniform results. The molecules given in Supplemental Table S1 were not extracted because of the high reliability of their changes; they also were not extracted because they were the most meaningful out of all those present in the reactions in the organism. In fact, the molecules were extracted because they constituted an overlapping portion of the low comprehensiveness of the proteomics with the comprehensiveness of the transcriptomics. Certainly, it is a type of important information, but it is not useful in terms of sensitivity of screening. Evidence exists that carrying out multiple omics analyses enables observation. For example, in this study, performing metabolomics made it possible to capture the metabolite change in the urea cycle. Figure 3 represents the metabolic and transcriptomic change in the urea cycle, mapped simultaneously on a KEGG metabolism map. There was no up-regulation in the urea cycle pathway. It was not possible to focus only on the urea cycle throughout the results of transcriptomics and proteomics, but being able to observe the metabolite change enabled the detection of a new change. The fact that there are aspects that can only be observed when multiple omics approaches are applied can be viewed as a disadvantage of using a single omics technique. However, in this context, multi-layered omics data should be interpreted with an understanding of its meaning, benefits, and limitations.

In contrast to the above results, the results for multi-layered omics approaches are not uniform. This section discusses the meaning of a non-uniform change. The transcriptomics and proteomics data given above reveal that they are almost non-uniform. While high correlation was observed between changes that were statistically significant, in almost all of the cases, one was not significantly different. The protein levels observed to be changed in the proteomics data were 15.1%, which were also observed to be changed in the transcriptomics data. From a reverse perspective, approximately 85% changes are specific to proteomics and are non-uniform between the two sets of omics data. In this case, when different results are derived from multiple omics, the differences in detection sensitivity—post-translation modification, oxidization of the protein, the stability of the protein, or metabolite—are the focus of debate and it is definitely true that such causes also play a large part. However, the essential meaning can be understood as the deviation in the time axis of the central dogma for each of the molecules. For example, in the case of molecule A and molecule B reacting to some kind of stimulus, the speed of the response to the stimulus and the speed of the transcription will differ. In the case of an immediate early gene, which rapidly responds to stimulus, the amount of mRNA will peak at an early stage after receiving the stimulus. However, a two-dimensional gene, which is transcriptionally controlled by some kind of transcriptional product, will slow down. In a study published in Nature, analysis of the speed of translation to protein was carried out on individual genes; the results showed that the speed of translation differed for each molecule [21]. Accordingly, for multiple omics data analyzed at the same time point it is impossible for all molecules to exhibit the same change. This is the paradox of multi-layered omics. Even though we tried to capture multiple stages of the biomolecule comprehensively, the fact that each molecule has a different speed means that it is impossible to comprehensively capture

the central dogma of the biomolecule.

However, this paradoxical aspect of multi-layered omics may actually be its largest benefit. If all molecules exhibited the same change, then there would be no need to use multiple omics. Precisely, because various molecules progress through the central dogma at differing speeds, it is extremely unlikely that the changes in all molecules would be uniform under multiple omics approaches and that the changes should not be uniform. This is why there is a necessity to use multiple omics analyses. The fundamental importance of using multiple omics approaches is not because it is possible to observe differing stages, it is because the time axis differs for each molecule that it is possible to capture the meaning of an organism which cannot be grasped using a single omics analysis.

5. Concluding Remarks

The present study reported the comprehensiveness of three omics analyses (transcriptomics, proteomics, and metabolomics) and the utility of using multiple omics analyses. Because comprehensiveness differs widely across these omics approaches, it is necessary to be aware of this when using multiple omics approaches. Furthermore, uniform changes were observed among changes at all stages but the majority of these specific to the omics approach. This data supports the fact that various molecules progress through the central dogma at differing speeds. Because the time axis differs for each molecule, combining multiple omics analyses makes it possible, for the first time, to investigate the reactions in organisms three-dimensionally. At first glance, it simply appears that combining a number of very large data sets produces even more complexity but, as discussed in this paper, if multi-layered omics data are treated with an awareness of their meaning, benefits, and limitations, then the combination of multiple omics analyses can be extremely useful for research in molecular biology. We hope that the knowledge shared in this paper can be of value in future research utilizing multiple omics analyses.

6. Supplementary material

Supplemental Figure S1. The food intake and the body weight of each group. (A) total food intake, (B) body weight.

Supplemental Table S1. The list of molecules that showed common changes between transcriptomics and proteomics.

References

1] G.A. Evans, Nat Biotechnol, 18 (2000) 127. doi: 10.1038/72480

2] G. N., Curr Opin Biotechnol., 13 (2002) 4

3] H. Kato, Asia Pac J Clin Nutr, 17 Suppl 1 (2008) 12-15

4] C. Has, J. Allmer, Information Sciences, (2016). doi: 10.1016/j.ins.2016.08.005

5] M. Schouten, P. Bielefeld, S.A. Fratantoni, C.J. Hubens, S.R. Piersma, T.V. Pham, R.A. Voskuyl, P.J. Lucassen, C.R. Jimenez, C.P. Fitzsimons, Sci Data, 3 (2016) 160068. doi: 10.1038/sdata.2016.68

6] F. Turroni, C. Milani, S. Duranti, L. Mancabelli, M. Mangifesta, A. Viappiani, G.A. Lugli, C. Ferrario, L. Gioiosa, A. Ferrarini, J. Li, P. Palanza, M. Delledonne, D. van Sinderen, M. Ventura, ISME J, 10 (2016) 1656-1668. doi: 10.1038/ismej.2015.236

7] D. Kumar, A.K. Yadav, X. Jia, J. Mulvenna, D. Dash, Mol Cell Proteomics, 15 (2016) 329-339. doi: 10.1074/mcp.M114.047126

8] E. Montague, I. Janko, L. Stanberry, E. Lee, J. Choiniere, N. Anderson, E. Stewart, W. Broomall, R. Higdon, N. Kolker, E. Kolker, Nucleic Acids Res, 43 (2015) D1145-1151. doi: 10.1093/nar/gku1175

9] M.P. van Iersel, M. Sokolovic, K. Lenaerts, M. Kutmon, F.G. Bouwman, W.H. Lamers, E.C. Mariman, C.T. Evelo, J Integr Bioinform, 11 (2014) 235. doi: 10.2390/biecoll-jib-2014-235

10] S. Takahashi, K. Egashira, K. Saito, H. Jia, K. Abe, H. Kato, Journal of Functional Foods, 6 (2014) 157-167. doi: 10.1016/j.jff.2013.10.002

11] R.A. Irizarry, B. Hobbs, F. Collin, Y.D. Beazer-Barclay, K.J. Antonellis, U. Scherf, T.P. Speed, Biostatistics, 4 (2003) 249-264. doi: 10.1093/biostatistics/4.2.249

12] K. Kadota, Y. Nakai, K. Shimizu, Algorithms Mol Biol, 3 (2008) 8. doi: 10.1186/1748-7188-3-8

13] H. Jia, W. Aw, M. Hanate, S. Takahashi, K. Saito, H. Tanaka, M. Tomita, H. Kato, Journal of Functional Foods, 11 (2014) 438-448. doi: 10.1016/j.jff.2014.09.018

14] H. Kato, Takahashi, S. and Saito K. J., Trad. Comp. Med., (2011) 6

15] T. Barber, J.R. Vina, J. Vina, J. Cabo, Biochem J, 230 (1985) 675-681

16] J.F. Cobbold, Q.M. Anstee, R.D. Goldin, H.R. Williams, H.C. Matthews, B.V. North, N. Absalom, H.C. Thomas, M.R. Thursz, R.D. Cox, S.D. Taylor-Robinson, I.J. Cox, Clin Sci (Lond), 116 (2009) 403-413. doi: 10.1042/CS20080159

17] N. Alcaraz, J. Pauling, R. Batra, E. Barbosa, A. Junge, A.G. Christensen, V. Azevedo, H.J. Ditzel, J. Baumbach, BMC Syst Biol, 8 (2014) 99. doi: 10.1186/s12918-014-0099-x

18] M. List, N. Alcaraz, M. Dissing-Hansen, H.J. Ditzel, J. Mollenhauer, J. Baumbach, Nucleic Acids Res, 44 (2016) W98-W104. doi: 10.1093/nar/gkw373

19] C. Mouse Genome Sequencing, R.H. Waterston, et al, Nature, 420 (2002) 520-562. doi: 10.1038/nature01262

20] D.S. Wishart, D. Tzur, C. Knox, R. Eisner, A.C. Guo, N. Young, D. Cheng, K. Jewell, D. Arndt, S. Sawhney, C. Fung, L. Nikolai, M. Lewis, M.A. Coutouly, I. Forsythe, P. Tang, S. Shrivastava, K. Jeroncic, P. Stothard, G. Amegbey, D. Block, D.D. Hau, J. Wagner, J. Miniaci, M. Clements, M. Gebremedhin, N. Guo, Y. Zhang, G.E. Duggan, G.D. Macinnis, A.M. Weljie, R. Dowlatabadi, F. Bamforth, D. Clive, R. Greiner, L. Li, T. Marrie, B.D. Sykes, H.J. Vogel, L. Querengesser, Nucleic Acids Res, 35 (2007) D521-526. doi: 10.1093/nar/gkl923

21] B. Schwanhausser, D. Busse, N. Li, G. Dittmar, J. Schuchhardt, J. Wolf, W. Chen, M. Selbach, Nature, 495 (2013) 126-127. doi: 10.1038/nature11848

JOURNAL OF INTEGRATED OMICS
A METHODOLOGICAL JOURNAL
HTTP://WWW.JIOMICS.COM

ORIGINAL ARTICLE | DOI: 10.5584/jiomics.v7i1.203

A novel extraction method for the preparation of heparinized chicken (*Gallus gallus domesticus*) and horse (*Equus caballus*) whole blood for ^{1}H -NMR metabolomics using Drabkin's reagent

Jennifer N. Niemuth*[1-3]; Michael K. Stoskopf.[1-3]

[1]Department of Forestry and Environmental Resources, College of Natural Resources, North Carolina State University, 2820 Faucette Dr., Raleigh, NC 27695, USA. [2]Department of Clinical Sciences, College of Veterinary Medicine, North Carolina State University, 1060 William Moore Drive, Raleigh, NC 27607, USA. [3]Environmental Medicine Consortium, North Carolina State University, 1060 William Moore Drive, Raleigh, NC 27607, USA.

Received: 19 October 2016 **Accepted:** 2 April 2017 **Available Online**: 12 April 2017

ABSTRACT

Despite the ease of collection, heparinized whole blood is underutilized in proton nuclear magnetic resonance spectroscopy-based metabolomics particularly because of the lack of sample homogeneity. Drabkin's reagent, an aqueous solution of potassium ferricyanide, potassium cyanide, and sodium bicarbonate, causes hemolysis and has been used for quantification of hemoglobin. The objectives of this study were to determine if the use of Drabkin's reagent with heparinized whole blood for metabolomics samples would result in consistent hemolysis, while being invisible to proton nuclear magnetic resonance spectroscopy and quenching metabolic activity. Heparinized whole blood from a chicken (*Gallus gallus domesticus*) and a horse (*Equus caballus*) was used. All heparinized whole blood samples were mixed 1:10 (volume:volume) heparinized whole blood:Drabkin's reagent. Lyophilized Drabkin's reagent rehydrated with a 100% deuterium oxide solution was invisible to proton nuclear magnetic resonance spectroscopy. Standard (10 min incubation, 20 min centrifugal filtration) and delayed (120 min incubation, 20 min centrifugal filtration) samples were prepared for both animal species. The only differences in spectra noted were minor differences in the amplitude of the major peaks of the metabolites 3-methylhistidine and betaine in the chicken samples. Comparison of standard and delayed samples via two-sample Kolmogorov-Smirnov tests found no significant differences between spectra for either animal species (chicken $p = 1$, horse $p = 0.9887$). Use of Drabkin's reagent resulted in consistent, complete hemolysis, while being invisible to proton nuclear magnetic resonance spectroscopy and quenching metabolic activity for at least 140 min at room temperature. This protocol should be considered when the investigator is interested in questions specific to erythrocyte metabolism and/or when heparinized whole blood is the only sample type available.

Keywords: *Equus caballus*; *Gallus gallus domesticus*; heparinized whole blood; metabolomic quenching; metabolomic sample handling; proton nuclear magnetic resonance spectroscopy.

Abbreviations: 1D: one-dimensional; ^{1}H: proton; D_2O: deuterium oxide; DR: Drabkin's reagent; Hb: hemoglobin; HWB: heparinized whole blood; K-S: Kolmogorov-Smirnov; NMR: nuclear magnetic resonance; TSP: trimethylsilyl propanoic acid; v:v: volume:volume.

1. Introduction

Biofluids, such as plasma, used in ^{1}H-NMR-based metabolomics studies provide a snapshot of the metabolic state of an organism. Advantages of biofluids, over most other tissues, include the relative ease of sample collection and low impact on patients or research animals, particularly when repetitive sampling is necessary. Biofluids also can often be analyzed via NMR with minimal to no sample preparation.

The application of metabolomics techniques to ecological questions where sampling wildlife may be necessary presents

***Corresponding author:** Jennifer N. Niemuth, North Carolina State University, College of Veterinary Medicine, Department of Clinical Science, 1060 William Moore Drive, Campus Box 8401, Raleigh, NC 27607, USA. Phone: +1-919-513-6230, Fax: +1-919-515-4237, E-mail Address: jennifer_niemuth@ncsu.edu

some special sample handling challenges over more routine clinical or laboratory settings. Particularly in the field, where electrical power and standard centrifuge use is often not practical, timely collection of plasma may not be possible. HWB is then a preferred sample. Measuring each HWB sample's hematocrit using battery powered minifuges or gravity methods allows the final spectral data to be normalized to the percentage of erythrocytes present in the blood. Unfortunately, the key first step of quenching the metabolism of metabolomics samples [1], commonly achieved in the field by immediate freezing with dry ice or liquid nitrogen, introduces variability to HWB samples because the amount of hemolysis induced in the freeze and/or thaw may not be consistent across samples.

Additionally, sedimentation and movement of intact erythrocytes during NMR analysis can complicate quality control [2,3]. A potential solution to these issues is to create homogeneous samples by completely hemolysing the sample, releasing all erythrocyte intracellular contents into the plasma.

Complete hemolysis of HWB samples for metabolomics also offers the opportunity to address research questions specifically about erythrocyte metabolism. For example, various metabolites, such as glutathione, have been shown to have much greater intraerythrocytic concentrations compared to plasma [4].

In a pilot study designed to evaluate possible methods for achieving reliable complete hemolysis of HWB, established solvents used in sample extractions for NMR metabolomics, such as chloroform and methanol, as well as other solvents, including deionized water, acetone, and ammonia, either did not produce complete hemolysis or physically changed the samples by greatly increasing viscosity, thereby inhibiting further manipulation (Niemuth, unpublished dataset). Chloroform, methanol, deionized water, and acetone were tested at 1:1, 2:1, 5:1, and 10:1 solvent:HWB sample (v:v). Ammonia was tested in a range of concentrations from 1 M to 14.8 M. Deionized water and ammonia less than 3 M did not produce complete hemolysis. Chloroform or ammonia greater than 3 M resulted in a gelatinous sample, while samples treated with methanol or acetone caused clumping. Physical disruption methods using various tissue homogenizers, lyophilization, and sonicators were inconsistent, required extensive time per sample, and increased sample temperature, which without a permanent quenching method could perturb the resulting metabolomes.

DR is a commercially available aqueous solution of potassium ferricyanide, potassium cyanide, and sodium bicarbonate developed for the cyanhemoglobin spectrophotometric method of quantitative Hb determination [5]. DR causes hemolysis and conversion of Hb to cyanmethemoglobin [6-8].

The objectives of this study were to determine if the use of DR with HWB for metabolomics samples would result in consistent hemolysis, while being invisible to ^{1}H-NMR and quenching metabolic activity. Heparinized chicken (Gallus *gallus domesticus*) and horse (*Equus caballus*) whole blood was employed to allow comparison of results with nucleated and non-nucleated erythrocytes, respectively.

2. Material and Methods

2.1. Biological samples and chemical reagent

HWB for this study was obtained from a horse and a chicken during routine clinical diagnostics and euthanasia, respectively. HWB was frozen after collection, stored at -80 °C, and thawed at room temperature (20-21 °C) before use. Commercially available DR (Ricca Chemical Company, Arlington, TX, USA) was used and the pH measured (accumet Basic AB15 Plus, Thermo Fisher Scientific, Inc., Waltham, MA, USA).

2.2. Determination of sample and reagent incubation time

To determine necessary incubation time, a HWB sample from chicken and horse was individually mixed 1:10 (v:v) HWB:DR. The absorbance of each sample was measured with a spectrophotometer (Nanodrop 1000, Thermo Fisher Scientific, Inc., Waltham, MA, USA) at 540 nm approximately every 5 min for a total of approximately 45 min. Plain DR was used as the blank for the spectrophotometer. Change in absorbance over time was used to determine the incubation time for the remainder of the study.

2.3. Determination of Hb extraction efficacy

To evaluate efficacy of Hb extraction, another HWB sample from each animal species was individually mixed 1:10 (v:v) HWB:DR. Both samples were incubated at room temperature for 10 min then centrifuged (3000 g; 5 min; room temperature). The supernatant was collected and saved (stored away from light at room temperature) until analysis. A new aliquot of DR was added to the HWB pellet, vortexed, and the incubation and centrifugation steps were performed as before. These steps were repeated until a total of 5 supernatants were collected from both samples. The absorbance of each supernatant was measured with a spectrophotometer at 540 nm. Change in absorbance over time was used to determine the efficacy of DR Hb extraction and the necessity of multiple washes per sample for the remainder of the study. A HWB chicken sample was also mixed 1:10 (v:v) HWD:DR, incubated (10 min; room temperature) and examined via light microscopy as air-dried, Wright's stained smears.

2.4. ^{1}H-NMR sample preparation

Amicon Ultra 10K 0.5 mL centrifugal filters (Millipore, Carrigtwohill, County Cork, Ireland) were prepared before

use by soaking in ultrapure water for a minimum of 8 h, washed 4 times with 0.5 mL ultrapure water (14,000 g; 20 min; room temperature), and stored in fresh ultrapure water if not used immediately (room temperature; used within 1 day). All samples were filtered prior to NMR analysis (14,000 g; 20 min; room temperature), including an aliquot of plain DR.

For chicken and horse samples, 40 µL HWB and 400 µL DR were mixed, incubated for 10 min at room temperature, and centrifuged (as above). The resulting filtrate was promptly frozen at -80 °C until lyophilization. Hereafter, these are referred to as standard samples. A second set of samples was prepared in the same manner, but was held at room temperature for 120 min prior to centrifugation. Hereafter, these are referred to as delayed samples. Frozen filtrates were lyophilized (-50 °C; FreeZone 2.5, Labconco, Kansas City, MO, USA) until dry (approximately 6 h), sealed with laboratory wax film (Parafilm, Beemis NA, Neenah WI, USA), and returned to -80 °C until NMR analysis.

Sealed lyophilized samples were thawed at room temperature. All samples were rehydrated with 70 µL D_2O with 20 mM phosphate buffer, 0.1 mM TSP, and 1 mM formate. Formate was used as second reference standard in case of interaction between TSP and plasma proteins [9]. Rehydrated samples were filtered (Fisherbrand SureOne 10 µL, extended, filter, low retention, universal fit pipet tips, Thermo Fisher Scientific, Waltham, MA, USA) via centrifugation (3,000 g; 2 min; room temperature) into vials and capped. For quality assurance, blank samples of the D_2O solution were run before and after each animal species' samples.

2.5. ^{1}H-NMR data collection, processing, and analysis

Samples were analyzed with a Varian Inova 600 MHz multinuclear INOVA NMR spectrometer (Varian Medical Systems, Palo Alto, CA, USA) equipped with a Protasis microcoil NMR probe (Protasis Corporation, Marlboro, MA, USA) to obtain 1D, ^{1}H-NMR spectra at 25 °C with a 1.1 sec acquisition time. The sweep width of 7,193 Hz acquired 8,189 complex points and 4,096 transients. Prior to insertion into the spectrometer, sample pH was measured and no practical differences in pH that would require adjustment of technique were noted.

NMR spectra were processed using ACD labs 12.0 1D NMR Processor (Advanced Chemistry Development, Toronto, Ontario, Canada). Spectra were zero-filled to 16,000 points and Fourier transformed. Spectral phasing and baselines were corrected automatically and adjusted, if necessary. All spectra were referenced to the internal standard TSP peak at 0 ppm. Peak identification was performed with Chenomx NMR suite 8.1 (Chenomx, Edmonton, Alberta, Canada) and the Human Metabolome Database [10].

Prior to statistical analysis, dark regions for each animal species were set to eliminate upstream/downstream areas without metabolites (including TSP peaks) and the water peak. Spectra for each animal species were grouped and intelligent bucketing was performed with a bin width of 0.04 ppm and 50% width looseness. This resulted in 214 and 204 bins for the chicken and horse samples, respectively. Integrals were normalized for each sample by dividing each bin value (i.e. integral) by the sum of the bins for that particular sample. Spectra for each animal species were compared statistically via a two-sample K-S test (two-sided, $\alpha = 0.05$) with R version 3.2.3[11].

3. Results

Measured pH of DR was 8.610. The alkaline pH of the samples did not appear to interfere with peak identification using reference spectra made with standard solvents.

Spectrophotometric evaluation of incubated DR treated samples revealed little change in absorbance after approximately 10-15 min. All samples thereafter were incubated for 10 min after DR addition before further processing, except where noted.

Absorbance of the second through fifth collected supernatants was decreased by >95% versus the initial supernatant. All samples thereafter were subjected to a single 1:10 (v:v) HWB:DR treatment to achieve extraction. The aliquot of the chicken sample used in this portion of the study developed a small gelatinous mass after DR treatment similar to what has been described in trout blood by Larsen and Snieszko [7]. The mass lightened in color after each subsequent DR aliquot. Examination via light microscopy of air-dried, Wright's stained smears resulted in subjectively uniform hemolysis.

DR was invisible to ^{1}H-NMR (Figure 1). Blank samples run prior to and after samples from each animal species did not demonstrate any contamination that carried over into the test samples. Standard and delayed samples for both animal species did not appear considerably different, either in regards to metabolite presence/absence or relative metabolite concentrations. Subjectively, the greatest difference appeared to be with the major peaks of the

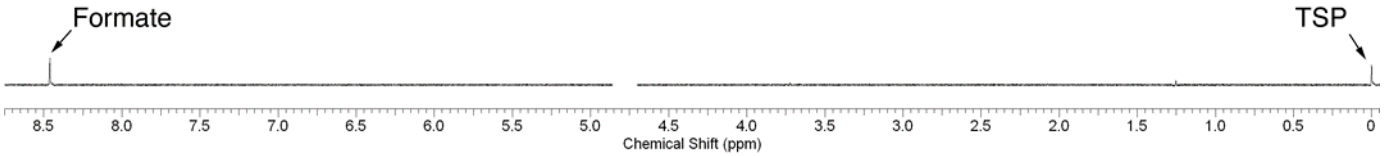

Figure 1. ^{1}H-NMR spectrum of filtered DR. The water peak has been deleted. TSP and formate were added to all samples as reference standards.

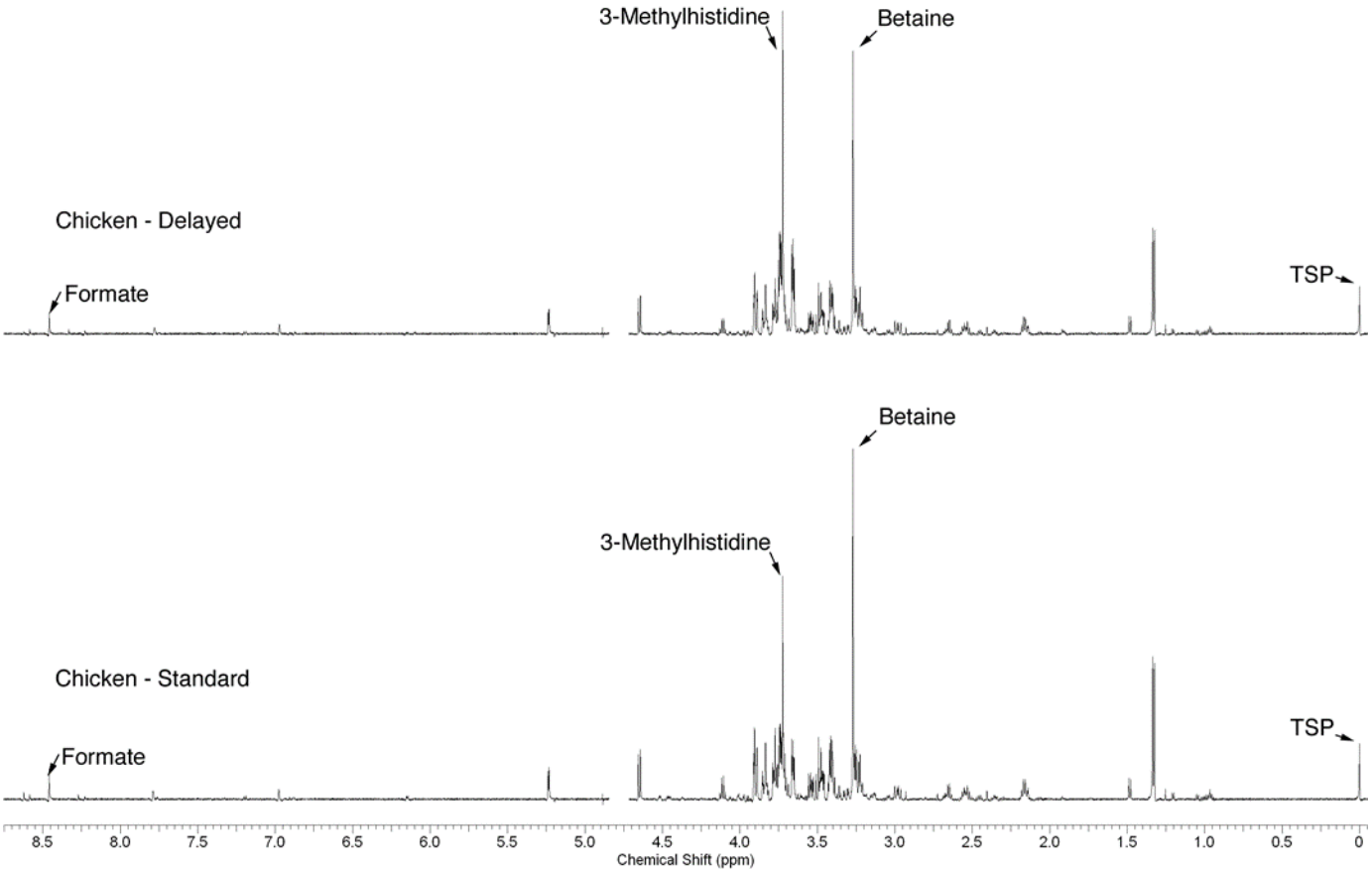

Figure 2. [1]H-NMR spectra of DR treated chicken HWB. The water peak has been deleted. The standard sample was incubated at room temperature for 10 min with DR prior to 20 min of centrifugal filtration. The delayed sample was incubated at room temperature for 120 min with DR prior to 20 min of centrifugal filtration. Subjectively, the greatest difference appeared to be with the major peaks of the metabolites betaine (singlet at approximately 3.3 ppm, methyl group protons) and 3-methylhistidine (singlet at approximately 3.7 ppm, methyl group protons with minor overlap contribution from components of a multiplet and doublet representing single protons on carbons 7 and 8, respectively).

metabolites betaine (approximately 3.3 ppm) and 3-methylhistidine (approximately 3.7 ppm) in the chicken samples (Figure 2). Both horse spectra were very similar (Figure 3). Provisional metabolite identifications and reference chemical shifts based on database comparisons are included as Table 1. Comparison of standard and delayed samples via two-sided, two-sample K-S tests found no significant differences with either animal species (chicken $p = 1$, horse $p = 0.9887$; both are approximate due to the presence of ties).

4. Discussion

The results of this study demonstrate that DR can be used as a component of an effective and simple extraction method for chicken and horse HWB samples for [1]H-NMR metabolomics. DR is commercially available, inexpensive, and has minimal storage requirements (protection from light, freezing, and contact with acids). The amount of potassium cyanide and potassium ferricyanide in 1 L of Drabkin's reagent is much lower than the lowest-observed-adverse-effect level for an average 70 kg human [12].

Depending on the investigator's metabolites of interest, the native pH of DR and the resultant HWB filtrate may require the development of a specific database for DR samples. With our spectra, we were able to identify metabolites using standard reference spectra with minimal to no chemical shift changes. However, the chemical shift of a particular metabolite could be influenced by pH as the molecule is protonated or deprotonated [13]. Titration to a more neutral intracellular pH could be a potential approach to allow peak identification for such metabolites using existing databases. For unknown metabolites, investigators may have success identifying chemical shifts through the calculation of titration curves [13]. However, caution should be exercised as the addition of acid to DR can release hydrogen cyanide [14]. The potential for pH differences between samples should also be considered, especially when studying any physiologic or disease condition resulting in acidosis or alkalosis of the patient [15]. Lastly, one may need to consider the body temperature of the animal species being studied and the temperature at which pH measurements are made. For example, in poikilothermic and ectothermic animal species, such as reptiles, it is necessary to apply a

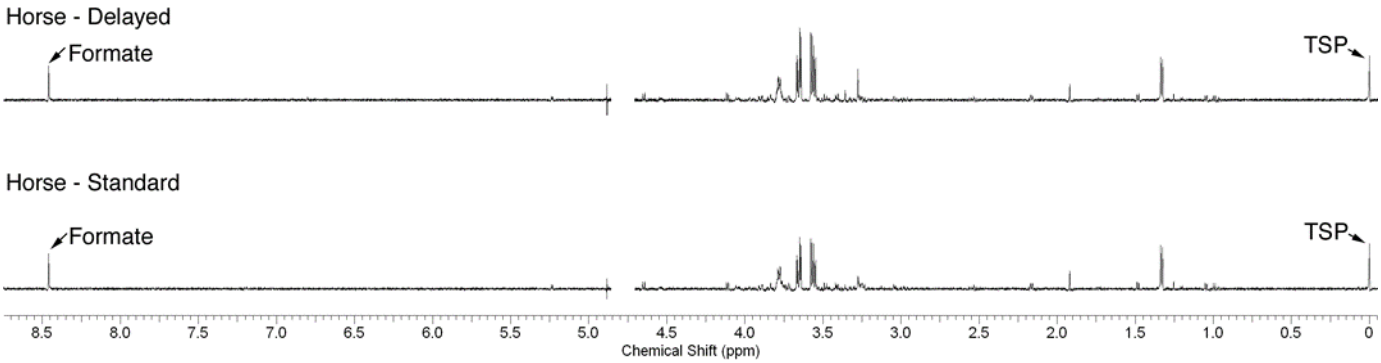

Figure 3. [1]H-NMR spectra of DR treated horse HWB. The water peak has been deleted. The standard sample was incubated at room temperature for 10 min with DR prior to 20 min of centrifugal filtration. The delayed sample was incubated at room temperature for 120 min with DR prior to 20 min of centrifugal filtration. Subjectively, both spectra appear very similar.

correction for the animal's body or environmental temperature to accurately evaluate many clinical measurements, including blood pH [16].

The incubation time of 10 min used in this paper is in agreement with a 5 to 10 min minimum reported in other published protocols for use of DR for hemolysis [5-7]. Hb is a large molecule with a diameter of approximately 5 nm and a total molecular weight of 64,000 Daltons [17]. Our metabolites of interest generally have molecular weights less than 10,000 Daltons. Therefore, we would expect that extraction of Hb from the erythrocyte would also allow for the release of intracellular metabolites. The results of evaluation of blood smears made from DR treated HWB suggested complete hemolysis. This was supported by the near complete extraction of Hb after a single application of DR.

The small gelatinous mass observed in one of the chicken samples during extraction testing was consistent with what has been described in trout [7]. The mass did not interfere with supernatant collection and while no masses were observed in the samples used for NMR analysis, they would have been removed by the filtration step. The formation of these masses has been noted when using DR for hemoglobin quantification and it has been recommended that they be removed (e.g. if within a spectrophotometer cuvette) with a wooden applicator stick [18].

Table 1. Provisional metabolite identifications and reference chemical shifts [10]. Absolute metabolite confirmation would require additional NMR experiments. (s: singlet, d: doublet, t: triplet, q: quartet, m: multiplet, dd: doublet of doublets, tt: triplet of triplets).

Metabolite	Chemical Shift (ppm) & Peak Shape	Chicken	Equine
3-Aminoisobutyrate	1.16-1.21 (d), 2.57-2.64 (m), 3.00-3.05 (dd), 3.06-3.16 (dd)	•	•
3-Hydroxyisovalerate	1.26 (s), 2.35 (s)	•	•
3-Methylhistidine	3.24 (m), 3.70 (s), 3.93 (dd), 7.05 (s), 7.92 (s)	•	
Acetate	1.91 (s)	•	•
Alanine	1.47 (d), 3.77 (q)	•	•
AMP	4.01 (dd), 4.36 (dd), 4.50 (dd), 6.12 (d), 8.23 (s), 8.58 (s)	•	
Betaine	3.25 (s), 3.89 (s)	•	•
Creatinine	3.03 (s), 4.05 (s)	•	•
Formate*	8.44 (s)	•	•
Glucose	3.233 (dd), 3.398 (m), 3.458 (m), 3.524 (dd), 3.728 (m), 3.824 (m), 3.889 (dd), 4.634 (d), 5.223 (d)	•	•
Glutathione	2.15 (m), 2.54 (m), 2.97 (dd), 3.78 (m), 4.20 (q)	•	•
Glycerol	3.551 (m), 3.644 (m), 3.775 (tt)		•
Inosine	3.832 (dd), 3.902 (dd), 4.257 (dd), 4.420 (dd), 4.798 (s), 6.055 (d), 8.187 (s), 8.305 (s)	•	
Lactate	1.32 (d), 4.10 (q)	•	•
Leucine	0.948 (t), 1.700 (m), 3.722 (m)	•	•
Methanol	3.34 (s)	•	•
Sarcosine	2.73 (s), 3.60 (s)	•	
Succinate	2.39 (s)	•	
Valine	0.976 (d), 1.029 (d), 2.261 (m), 3.601 (d)	•	•

One of the main reasons for selecting DR versus other commercially available hemolysis agents was that we hypothesized DR would be NMR-friendly, expecting lyophilization to remove the only protons in the solution. ^{1}H-NMR analysis of filtered and lyophilized DR confirmed that DR is invisible (Figure 1).

Visually there were only subtle differences in singlet peak amplitudes between the standard and delayed chicken sample spectra. 3-Methylhistidine is an aromatic heteromonocyclic related to muscle breakdown [10], while betaine is involved in glycine, serine, and threonine metabolism [19]. We are not able to determine if the differences in 3-methylhistidine and betaine are due to true sample change or are the result of some other unidentified variability. The Kolmogorov-Smirnov test is used to detect differences in location and shape and did not indicate that either the chicken or horse standard or delayed samples were from different distributions. If it is anticipated that a delay greater than the 20 min necessary for centrifugal filtration will be a required part of a study protocol, it would be prudent to run test samples to determine what, if any, metabolites may be impacted.

5. Concluding Remarks

Use of DR with chicken and horse HWB for metabolomics resulted in consistent, complete hemolysis, while being invisible to ^{1}H-NMR and quenching metabolic activity for at least 140 min at room temperature. This protocol was equally effective with nucleated and non-nucleated erythrocytes of the chicken and horse, respectively, and should be considered when HWB is the only sample type available and/or if the investigator is interested in questions specific to erythrocyte metabolism.

Acknowledgments

This study was funded by a grant from the Bernice Barbour Foundation, Inc. The authors thank Drs. Scott Bailey and Luke Borst for providing blood samples, the Macdonald laboratory and the University of North Carolina Metabolomics Facility at The Hamner Institutes for Health Sciences for use of their magnet, and Dr. Jennifer Neel for her advice on hemolysis determination.

References

1] M.R. Viant, C. Ludwig, U.L. Günther, in: W.J. Griffiths (Ed.), Metabolomics, Metabonomics and Metabolite Profiling, The Royal Society of Chemistry, Cambridge, UK, 2008, pp. 44-70.

2] F.F. Brown, I.D. Campbell, P.W. Kuchel, FEBS Lett, 82 (1977) 12 -16. DOI: 10.1016/0014-5793(77)80875-2

3] J.K. Nicholson, M.J. Buckingham, P.J. Sadler, Biochem J, 211 (1983) 605-615. DOI: 10.1042/bj2110605

4] M.D. Rosenthal, R.H. Glew, Medical Biochemistry: Human Metabolism in Health and Disease, John Wiley & Sons, Inc., Hoboken, New Jersey, USA, 2009.

5] D.L. Drabkin, J.H. Austin, J Biol Chem, 98 (1932) 719-733. http://www.jbc.org/content/98/2/719.short

6] S.M. Lewis, S. Kumari, Guidelines on Standard Operating Procedures for Haematology, http://apps.searo.who.int/PDS_DOCS/B0215.pdf, Accessed 2016.

7] H.N. Larsen, S.F. Snieszko, Fish culture, 23 (1961) 8-17. DOI: 10.1577/1548-8659(1961)23[8:COVMOD]2.0.CO;2

8] J. Samour, in: G.J. Harrison, T.L. Lightfoot (Eds.), Clinical avian medicine, first ed., Spix Publishing, Palm Beach, FL, 2006, pp. 587-609.

9] M. Kriat, S. Confort-Gouny, J. Vion-Dury, M. Sciaky, P. Viout, P.J. Cozzone, NMR Biomed, 5 (1992) 179-184. DOI: 10.1002/nbm.1940050404

10] D.S. Wishart, C. Knox, A.C. Guo, R. Eisner, N. Young, B. Gautam, D.D. Hau, N. Psychogios, E. Dong, S. Bouatra, R. Mandal, I. Sinelnikov, J. Xia, L. Jia, J.A. Cruz, E. Lim, C.A. Sobsey, S. Shrivastava, P. Huang, P. Liu, L. Fang, J. Peng, R. Fradette, D. Cheng, D. Tzur, M. Clements, A. Lewis, A. De Souza, A. Zuniga, M. Dawe, Y. Xiong, D. Clive, R. Greiner, A. Nazyrova, R. Shaykhutdinov, L. Li, H.J. Vogel, I. Forsythe, Nucleic Acids Res, 37 (2009) D603-D610. DOI: 10.1093/nar/gkn810

11] R Core Team, R: A language and environment for statistical computing, http://www.R-project.org/, Accessed 2016.

12] Agency for Toxic Substances and Disease Registry (ATSDR), Toxicological profile for Cyanide, U.S. Department of Health and Human Services, Public Health Service, Atlanta, Georgia, USA, 2006.

13] G.P. Kreishman, E. Brooks, in: R.S. Macomber (Ed.), A complete introduction to modern NMR spectroscopy, First ed., John Wiley & Sons, Inc., New York, New York, USA, 1998, pp. 252-282.

14] Ricca Chemical Company, Safety Data Sheet - Drabkin's Reagent, http://www.riccachemical.com/Technical-Support/MSDS/2660, Accessed 2016.

15] O. Beckonert, H.C. Keun, T.M.D. Ebbels, J. Bundy, E. Holmes, J.C. Lindon, J.K. Nicholson, Nat Protocols, 2 (2007) 2692-2703. DOI: 10.1038/nprot.2007.376

16] C.A. Harms, K.M. Mallo, P.M. Ross, A. Segars, J Wildl Dis, 39 (2003) 366-374. DOI: 10.7589/0090-3558-39.2.366

17] H.P. Erickson, Biol Proc Online, 11 (2009) 32-51. DOI: 10.1007/s12575-009-9008-x

18] P. Blaxhall, K. Daisley, J Fish Biol, 5 (1973) 771-781. http://dx.doi.org/10.1111/j.1095-8649.1973.tb04510.x

19] M. Kanehisa, Y. Sato, M. Kawashima, M. Furumichi, M. Tanabe, Nucleic Acids Res, 44 (2016) D457-D462. DOI: 10.1093/nar/gkv1070

JOURNAL OF INTEGRATED OMICS
A METHODOLOGICAL JOURNAL
HTTP://WWW.JIOMICS.COM

ORIGINAL ARTICLE | DOI: 10.5584/jiomics.v7i1.195

Identification of NEK3 interacting proteins and phenotypical characterization of its silencing in HeLa cells

Vanessa Bomfim Cardoso[1,2], Talita Diniz Melo-Hanchuk[1], Edmarcia Elisa de Souza[1], Priscila Ferreira Slepicka[2], Gabriela Vaz Meirelles[2], Jörg Kobarg[1,3]*

[1]Department of Biochemistry and Tissue Biology – Graduate Program in Functional and Molecular Biology, Biology Institute, State University of Campinas, Campinas, Sao Paulo, Brazil. [2]Brazilian Biosciences National Laboratory, Brazilian Center For Research in Energy and Materials, Campinas, Sao Paulo, Brazil. [3]Faculty of Pharmaceutical Sciences, State University of Campinas, Campinas, Sao Paolo, Brazil.

Received: 11 February 2016 **Accepted:** 18 April 2017 **Available Online:** 06 May 2017

ABSTRACT

NEKs (NIMA-related kinases) are a group of kinases that share high amino acid sequence identity to NIMA (Never in mitosis gene A), which exists as a single member in the fungi *Aspergillus nidulans* and is functionally involved in the initiation of mitosis. NEK3 is a 506 amino acid serine/threonine kinase, localizes both to the nucleus and cytoplasm, and has an N-terminal catalytic domain and a C-terminal regulatory domain. NEK3 is also involved in cell motility and invasiveness of breast cancer tumor cells through interaction with regulators of the Rho GTPases Rac1 and RhoA, mediated by prolactin induced association of NEK3 to the human Prolactin Receptor (PRLR). A screening for interaction partners was performed and 27 different proteins were found. The identified candidate interacting proteins are functionally involved in processes, which are related with the most important steps of cancer progression and can be used to understand NEK3 function and behavior. One of the most important cytoplasmic NEK3 interactors is RhoGDI2 (RhoGDP-dissociation inhibitor 2). RhoGDI2 as well as VAV2, are regulators of RhoGTPases and inhibit Rac1 and RhoA activation with effects not only in bladder cancer, but also promotes invasion of breast cancer cells. Another GTPase, RhoA, is the main component of the cleavage furrow and is required for proper cytokinesis. In this respect, NEK3 was found in the furrow of ingression and its depletion is associated to cytokinesis delay due to DNA bridges, that is related to aneuploidy, tetraploidy, micronuclei. Also, NEK3 has a role in the promotion of tubulin acetylation, which in turn suggest that the role for NEK3 in DNA bridge formation may be related to microtubule stabilization and consequently, chromosomal instability. According to this, NEK3 also has a role in cell cycle regulation, which help to elucidate one of the roles for NEK3 in cancer.

Keywords: NEK3, Kinases, Yeast Two-Hybrid Screening, RhoGDI2, RhoA.

Abbreviations: NEK3: NIMA-related kinase 3; RhoGDI2: RhoGTPase dissociation inhibitor 2; VAV2: Guanine Exchange Factor 2; HEK293T: Human Embryonic Kidney 293T; GEF: Guanine Exchange Factor; GAP: GTPase Activating Protein; GDI: Guanosine nucleotide dissociation inhibitors; GFP: Green Fluorescent Protein. PIAS1: Protein Inhibitor of Activated STAT 1, SGIP1: SH3-containing GRB2-like protein 3-Interacting Protein 1, CNTN1: Contactin-1, FBN1: Fribrilin-1, MED17: Mediator of RNA polymerase II transcription subunit 17, PA2G4: Proliferation-associated protein 2G4 e COMMD1: COMM domain-containing protein 1.

1. Introduction

NEKs (NIMA-related kinases) are a group of kinases that share high amino acid sequence identity to NIMA (Never in mitosis gene A), which exists as a single member in the fungi *Aspergillus nidulans*, functionally involved in the initiation of mitosis. NIMA is a 79 kDa protein with an N-terminal kinase domain and a C-terminal regulatory domain rich in regulatory motifs: Coiled-coil domain, responsible to mediate protein-protein interactions (as in Nek1 and Nek9) and possibly its dimerization (as found -at least for: Nek1, Nek2, Nek9); and two PEST sequences related to regulated protein degradation [1–4]. Activation of this serine/threonine kinase at the G2/M transition of the cell cycle is required for entry into mitosis. Upon deletion of the gene encoding NIMA, cells

***Corresponding author:** Jörg Kobarg, Institute of Biology, Departamento de Bioquímica e Biologia Tecidual, University of Campinas-UNICAMP, 13083-862 Campinas, SP, Brazil; E-mail address: jorgkoba@unicamp.br, phone +55-19-3521-1443

arrested in G2, whereas when the protein was over-expressed the cells were driven into mitosis from any point in the cell cycle [2,4–8].

Most of the 11 mammalian NEKs already studied, are functionally related to NIMA but some degree of neo-functionalization also took place. Aside their participation in the context of NIMAs function in cell cycle progression and regulation, we can further annotate Neks in associated roles with a) centrosome disjunction b) primary cilia function and c) DNA damage response checkpoints and regulation of repair pathways [9].

Failure from cell cycle checkpoints results in genomic instability (GIN), a cellular state that leads to an increase in genetic alterations which are classified by: nucleotide instability and chromosomal instability (CIN). Among the causes leading to genomic instability, CIN is the most common. The main consequence of CIN is aneuploidy, that for decades has been related to tumorigenesis [10]. It has been reported that both aneuploidies and DNA alterations (mutation, chromosomal translocation and gene amplification) result in cell heterogeneity, which in turn support tumor adaptation environmental changes, a hallmark of human cancer [11–13].

So far, it is known that the role of NEKs in genomic stability goes beyond their participation in DNA repair. NEK2, due to serine phosphorylation of Hec1, promotes the proper chromosome segregation [14,15]. Cells from NEK1 knockout mice presented errors in DNA repair associated with breakage and irregular size of chromosomes, chromosome lagging and aberrant cytokinesis, which reinforce its role in checkpoint DNA repair. NEK1 knockout cells also presented polyploidy after only a few passages, as a consequence of aberrant cytokinesis [16].

NEK3 is a 506 amino acid long serine/threonine protein kinase that localizes both in the nucleus and cytoplasm [17,18] and which gene localizes to 13q14.2 chromosome. Structurally, NEK3 has an N-terminal catalytic domain and a C-terminal regulatory domain which contains residue Thr475 in its PEST domain that is phosphorylated upon activation [19]. Expression of mutant NEK3 without Thr475 or PEST domain causes changes in cellular morphology and polarity of neuronal cells [20].

Functionally, NEK3 is also involved in cell motility and invasiveness of breast cancer tumor cells through interaction and possibly direct phosphorylation of VAV2, a GEF type regulator of the Rho GTPases. VAV1 and VAV2 are regulators of Rac1, Cdc42 and RhoA GTPases. Proteins of this family are molecular switches that alter between active

Figure 1: The role of NEK3 in prolactin signaling pathway. NEK3 interacts with prolactin receptor (PRLR) and VAV2. Active Vav2 is a GEF for Rac1 and leads to its activation (Rac-GTP). This in turn activates Stat5 that promotes transcriptional activation of several genes in the nucleus that lead to the inhibition of apoptosis, cell proliferation, differentiation and in gall bladder cancer cells to diminished metastatic potential. Adapted from McHale, [42].

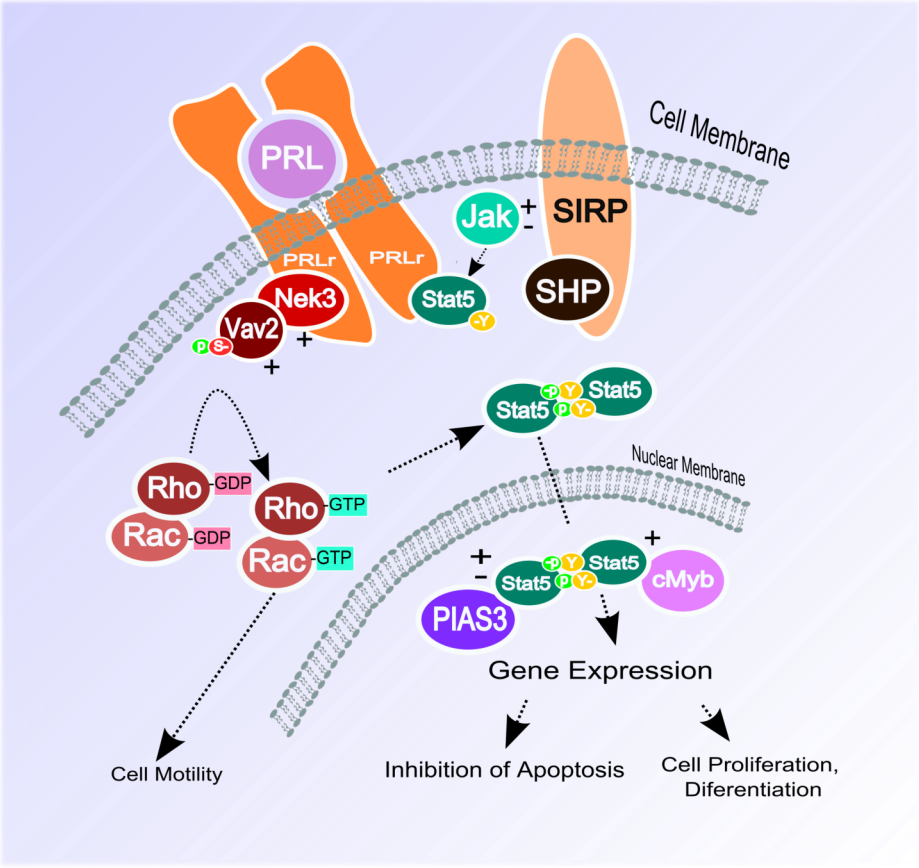

(bound to GTP) and inactive states (bound to GDP) and have key functions in cancer cell proliferation, apoptosis/ survival, cell polarity, cell adhesion and plasticity of cell migration [21,22]. A clear connection can be established between Rho proteins over-expression and a large variety of human tumors [23,24]. In turn, Rac1 is described to be involved in prolactin receptor and NEK3 mediated signaling [17] (Figure 1). In this context, the association of NEK3 to the intracellular domain of the human Prolactin Receptor after extracellular binding of the prolactin hormone to its receptor, possibly results in the activation of NEK3. VAV2 on the other hand has been shown to activate RhoGTPase Rac1, leading to activation of the Stat pathway and ultimately causing gene transcription activation in the nucleus [25,26].

In cell proliferation, RhoGTPases contribute through cell cycle progression, which depends on cyclin-dependent protein kinases which activity increases and decreases periodically during the growth and division of cells [27]. RhoA, for example, plays a role during cytokinesis leading to the contraction of the actin ring, through myosin light chain phosphorylation. Once the midbody is formed, RhoA must be inactivated since its excess may cause abscission arrest [53]. Also, to ensure proper cytokinesis progression, RhoA´s cortical localization must be controlled spatially and temporally [54].

In the present study, we identified several new interaction partners for NEK3 by a yeast two hybrid assay, that are related to processes involved in cancer progression and aggressiveness through GTPases regulation. Our experiments suggest that NEK3 has also a role in the cell cycle, specifically in cytokinesis since its suppression is related to DNA bridge formation and consequent delay in cytokinesis.

2. Material and Methods

2.1. Yeast Two-Hybrid Screening

Protein-protein interactions are highly important to understand the role of the protein in cellular context. We cloned the full-length NEK3 wild type cDNA in fusion with the GAL4 DNA Binding Domain (GAL4-BD) in pGBKT7 vector, which also contains *TRP1*, a selection marker for auxotrophic growth. This construct was transformed into Y2H Gold *Saccharomyces cerevisiae* yeast strain that contains heterologous genes *AUR1-C, HIS3, ADE2*, and *MEL1* under GAL4 transcriptional factor control. Another *S. cerevisiae* yeast strain, Y187, contains heterologous genes l*acZ* and *MEL1* previously transformed with the Universal Human (Normalized) cDNA Library constructs in pGADT7 -RecAB with *LEU2* expression marker gene and GAL4 DNA Activation Domain (GAL4-AD). These two haploid yeast strains were mated and plated on a selective quadruple dropout medium containing also Aureobasidin A and X-α-Gal (QDO-XA). Positive blue colonies indicated that proteins were expressed and interacted with Nek3 to reconstitute the functional complete GAL4 transcription factor.

2.2. Confirmation of Positive Interactions

After sequencing and BLAST analysis, *S. cerevisiae* strains were co-transformed with both pGBKT7-NEK3 and pGADT7-prey according to Yeastmaker™ Yeast Transformation System User Manual. The positive control (pGBKT7-p53 and pGADT7-T) and negative control (PGBKT7-Lam and pGADT7-T) were also co-transformed. Blue colonies were compared to control and determined to confirm positive interactions.

2.3. Integrated Interactome System – IIS

Blue colonies from yeast two-hybrid screening were sequenced, processed and integrated to annotated interaction networks using the "Integrated Interactome System" developed at the National Laboratory of Biosciences and State University of Campinas, Brazil (http://bioinfo03.ibi.unicamp.br/lnbio/IIS2/) [28]. Biological processes and cellular components were obtained from the Gene Ontology database (http://www.geneontology.org) integrated to IIS. The enriched biological processes from the Gene Ontology GO database were calculated in each network using the hypergeometric distribution [28]. The final layout and cellular component allocation were obtained with the Cytoscape online software [29] and the CellNetVis software (http://www.lge.ibi.unicamp.br/cellnetvis).

2.4. Analysis of NEK3-depletion phenotypes by short hairpin RNA

Viral transduction was performed using the lentiviral system with short-interfering rRNAs (shRNAs) designed for NEK3 (shRNA-Nek3.1: TRCN0000001471, 5'-GCAGTCCCATAGAACAGAAAT-3', for CDS of NEK3); (shRNA-Nek3.2: TRCN0000001473, 5'-CGAAGCATAACACACCAAGAA -3', for 3'UTR of NEK3). shRNA-GFP was used as a control plasmid. shRNAs sequences were obtained from The RNAi Consortium (TRC, IRB-Barcelona). Lentiviral particles were transduced with 1μg/mL polybrene in HeLa cells and stable lines were selected with puromycin 3μg/mL.

HeLa cells or HeLa stable cell line of shRNA-GFP, shRNA -Nek3.1 or shRNA-Nek3.2 were cultivated onto coverslips in 6-well plate for immunofluorescence assay under incubation in a humidified chamber at 37ºC with 5% CO2 in Dulbecco´s modified Eagle´s medium, DMEM (Gibco), supplemented with 10% certified fetal bovine serum (Gibco) and penicillin/streptomycin (100 units/mL, Gibco). All cells were mycoplasma tested regularly and before all experiments were proceeded.

Cells were fixed with ice-cold 100% methanol for 30 min,

Figure 2: NEK3 yeast two-hybrid interactome network and subcellular localization. (A) Most of the NEK3 interactors are localized in the nucleus, cytosol and plasma membrane. (B) The main cellular processes associated to NEK3 interactors. The enriched biological processes from the Gene Ontology GO database were calculated in each network using the hypergeometric distribution [28].

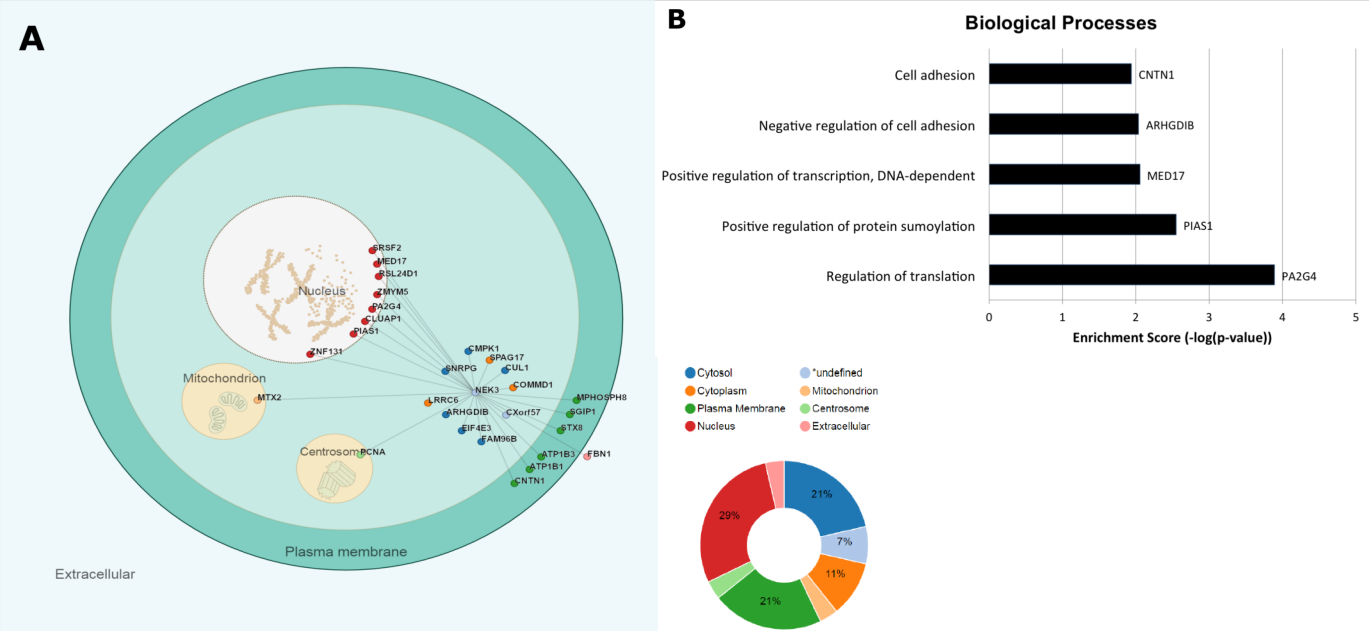

gently washed with 1xPBS (Phosphate buffer saline) and fixed specimens were permeabilized and blocked for 30 min at room temperature in blocking solution containing 1% BSA; 0.5% Triton X-100 into PBS.

Cells were incubated for 1 hour with the following primary antibodies diluted in blocking solution: rabbit anti-β-Tubulin (1:1000; ab15568; Abcam); rabbit Nek3 (1:200; AP8075C; Abgent); mouse RhoA; sc-418; Santa Cruz Biotechnology), all diluted in blocking solution. Next, the cells were incubated for 40 min in secondary fluorescent-labeled antibody: chicken anti-rabbit Alexa Fluor 488; chicken anti-mouse Alexa Fluor 647 (Life Technologies) diluted in blocking solution for concentration of 1:500. DNA was stained with Hoechst 33258 dye and coverslips were mounted on glass slides using ProLong Gold mounting media (Life Technologies).

Image data were collected in a Zeiss LSM 780 NLO Confocal Microscope (Carl Zeiss AG, Germany) using 40X or 100X lens. Series of Z stack images were captured from 0.7 µm thick sections and the entire cell volume was processed for 3-D rendering using Imaris (Bitplane). The numbers of HeLa cells were manually counted under a fluorescence microscope Leica DM2500 (Leica Microsystems). Statistical analysis was performed by the Student t-test and graphics plotted using GraphPad Prism software.

3. Results and Discussion

3.1. The construction of a NEK3 protein interaction map

The *in silico* analysis at the IIS and BLAST search resulted in 27 different proteins (Supplementary Table S1). The identified candidate interacting proteins are functionally involved in sumoylation, ubiquitinylation, transcriptional regulation, RNA processing, and the regulation of cell proliferation. A yeast co-transformation assay with NEK3-pGBKT7 and the prey proteins analyzed by the *Integrated Interactome* System was performed and, from 27 proteins initially found, some had their interaction confirmed in the yeast two-hybrid system itself like PIAS1, CNTN1, MED17 (CRSP77), PA2G4 (EBP1) (Supplementary Figure S1).

Using the Cytoscape software and CellNetVis, the Nek3 protein and its interaction network with subcellular localizations were performed (Figure 2A). Some interaction partners for NEK3 are mostly localized to the nucleus (29%) such as MED17 and PIAS1, but also to cytosol and to the cell membrane (21%). Importantly, the preys localized to the cell membrane are lipid anchored proteins or attached proteins, such as VAVs and SGIP1, which thus are proteins oscillating between the plasma membrane and cytosolic localizations.

One of the most expected Nek interactors, from the signaling context of Nek3, was RhoGDI2 / ARHGDIB (RhoGDP-dissociation inhibitor 2) (Figure 2). RhoGDI2 as well as VAV2, are negative regulators of the RhoGTPases Rac1 and RhoA which has been reported to suppress metastasis in bladder cancer, but also increased invasion of breast cancer cells [20]. A biphasic expression pattern of RhoGDI2 itself in breast cancer was found, where a correlation of its decreased expression in lymph node metastasis was reported [21]. Furthermore, another work found RhoGDI2 expression was up-regulated in human ovarian tumors of different histological subtypes [22]. These findings suggest that RhoGDI2 biology in cancer may depend on its interaction partners, including NEK3. RhoGDI2 may be alongside VAV2 and Rac1/RhoA an

additional new player in the signaling pathways regulated through the PRLR/Nek3.

PIAS1 (protein inhibitor of activated STAT-1) is an important component of SUMO (small ubiquitin modification protein) complex and acts as an E3 ubiquitin ligase adding SUMO to the substrate [30]. Recent works have shown that SUMOylation is also involved with Ran GTPase regulation and has important functions in nuclear traffic at interphase and mitotic spindle assembly [31]. The interaction between Nek3 and PIAS1 raise the possibility of an involvement of Nek3 in the SUMOylation process.

MED17 (CRSP77) is a member of mediator complex, a co-activator involved in transcription regulation of almost all RNA polymerase II-dependent genes. MED17 works as a bridge to transmit information from gene-specific regulatory proteins to RNA polymerase II transcription basal machinery. In this regard, MED17 is recruited by promotors through direct interactions with regulatory proteins and acts as a scaffold of pre-initiation complex with RNA polymerase II and its transcription factors [24]. Jeon and colleagues demonstrated for the first time a possible involvement of Neks in transcription. NEK6 phosphorylate STAT3 on Ser727 affecting the maximal transcription of a cancer cells [32].

Proliferation-associated protein 2G4 (PA2G4) or ErbB3-binding protein 1 (EBP1), is a modulator of the ErbB-3 transduction pathway – member of Epidermal Growth Factor (EGF) family – by interaction with its cytoplasmic domain [25]. EBP1 is also involved in first and late steps of RNA processing by association to 28S, 18S e 5.8S rRNA subunits [27].

Contactin1 (CNTN1) is a cell adhesion GPI-anchored protein, belonging to immunoglobulin superfamily [33]. This protein associates with other cell surface proteins like L1 or NCAM via homophylic interactions, and acts in signal transduction in neurons [34]. Contactin 1 is also related to invasion and metastasis in lung adenocarcinoma by RhoA activation [35], and its suppression increases cancer cell invasion and metastasis [24].

All for all, the NEK3 preys were related to a variety of processes involving cancer progression and aggressiveness, from cell cycle regulation to cell migration and invasion. Since molecular interactions help us to understand protein function and behavior, we can propose a complex role for NEK3 in different steps of cancer development.

Figure 3: Localization of NEK3 during cytokinesis of HeLa cells. Confocal images showing NEK3 accumulation at the furrow of ingression during anaphase (A) and at the midbody ring along with RhoA during cytokinesis (B). Images are presented as maximal intensity projections of multiple z-slices. Scale bar is indicated in the images (A: 5 μM, B: 10 μM). At least 170 randomly selected anaphase or cytokinesis cells were observed and all analyzed cells showed the NEK3 localization pattern represented in the images.

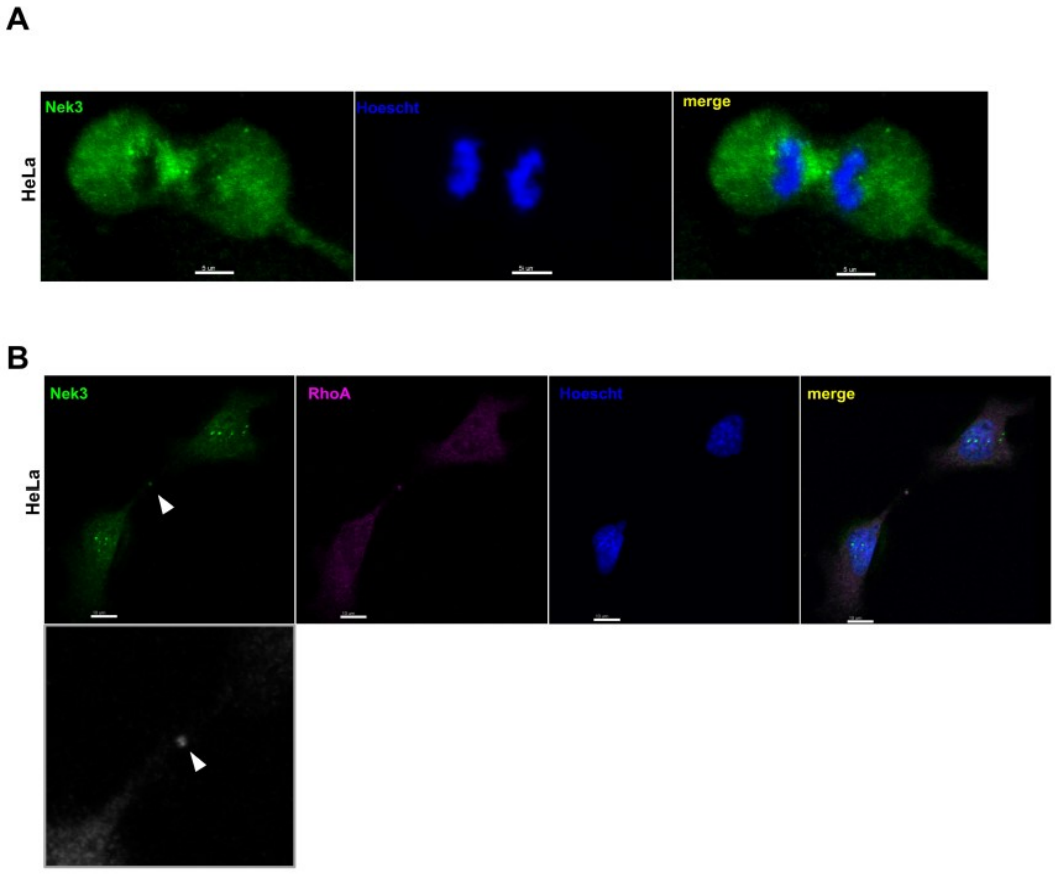

3.2. Study of cell cycle phenotypes in NEK3 knock-down HeLa cells

Formation of the mitotic cleavage furrow is dependent upon both microtubules and activity of the small GTPase RhoA [36]. Since NEK3 interact with RhoA we raised the hypothesis that NEK3 may have functions during cell division.

To explore this idea, we characterized the localization of NEK3 during cytokinesis. To this end, HeLa cells were stained for immunofluorescence of β-tubulin and NEK3 and analyzed by confocal microscopy. NEK3 was found enriched at the furrow of ingression during anaphase (Figure 3A), and at the midbody along with RhoA (Figure 3B) during cytokinesis pointing to their potential functional interplay during cell division.

These results led us to further investigate functional roles of NEK3 during cytokinesis. For this purpose, we employed lentivirus-delivered NEK3 silencing by RNAi in HeLa. The NEK3 suppression resulted in cytoplasmic bridges containing DNA (Figure 4A) Accordingly, there was an increase in the frequency of cells blocked in cytokinesis under these conditions indicating that NEK3 suppression delays cells at cytokinesis (Figure 4B). The cytokinesis delay due to DNA bridges may be related to aneuploidy, tetraploidy and micronuclei formation, which can lead to

Figure 4: Nek3-depletion induces DNA bridges during cytokinesis. (A) Confocal images show bridges containing DNA connecting the cells. DNA bridge are indicated by arrowheads in the images and enlargements of the cytoplasmic bridge region. Images are presented as maximal intensity projections of multiple z-slices in 3D rendering. Scale bars (lower row: 10 μM or 15 μM in the upper two rows) are indicated in the images. HeLa cells were counted through the microscope, and plotted in the graphic (right) using GraphPad Prism software . At least 65 cytokinesis cells per condition were counted in each duplicated of two independent experiments. *P<0.05 was considered as statistically significant. (B) Nek3-depleted cells delay for completion of cytokinesis**.** The number of HeLa cells were manually counted through the fluorescence microscope from immunofluorescence coverslips and plotted in the graphic. More than 400 cells per condition were counted in each duplicate of two independent experiments. Graphs were created and analysis of statistical significance was performed by the Student t-test using GraphPad Prism software. *P<0.05= statistically significant.

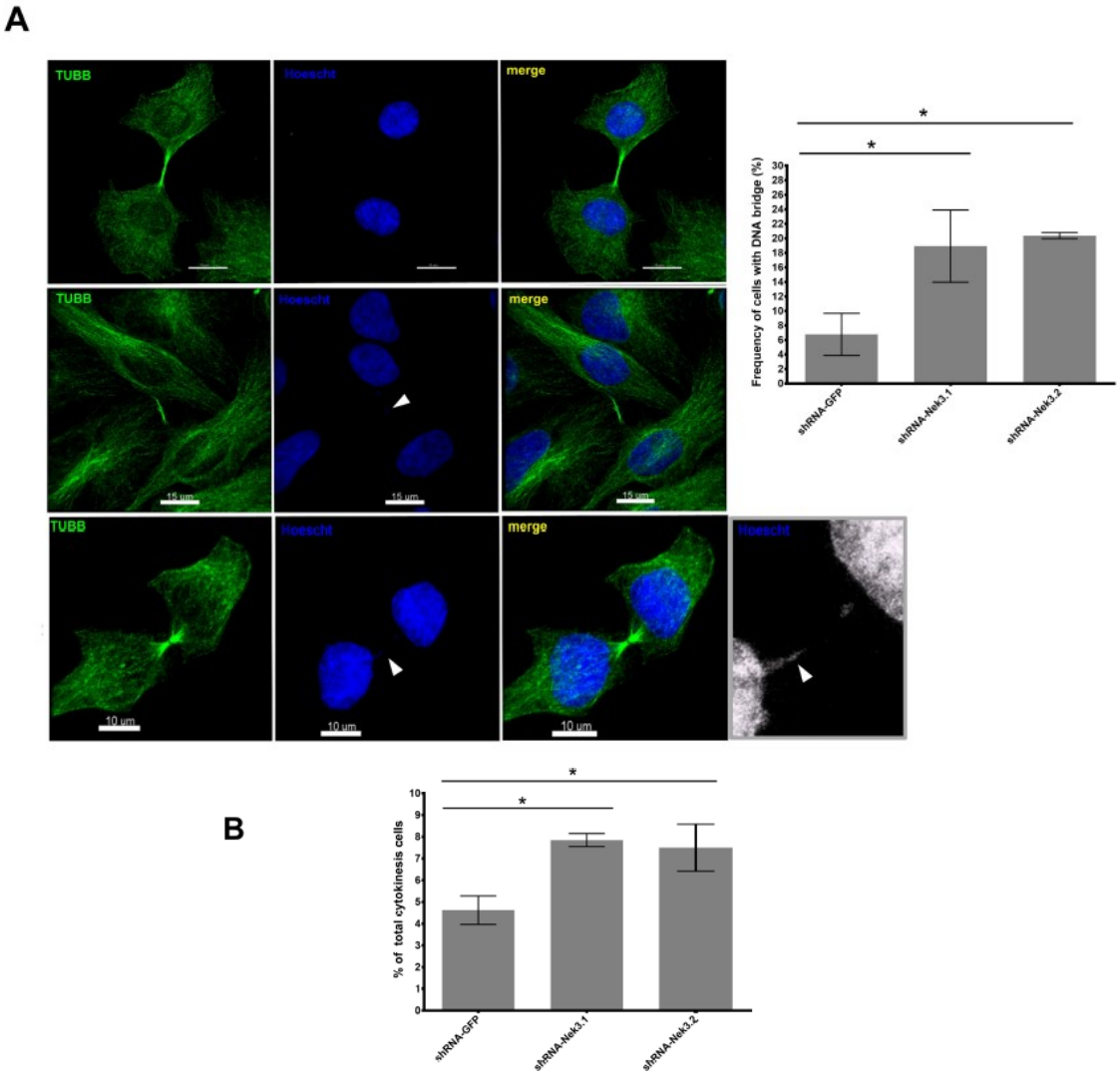

both cancer mutations and chromosomal instability [37].

Some interactors for NEK3 found in its yeast two hybrid assay are also related to the observed cell cycle phenotypes. Cullin 1 is involved in ubiquitination, degradation pathway that regulate proteins which controls cell division by two complexes: SCF and APC. This NEK3 partner together with SKP1, RBX1 and F-Box forms the SCF complex, which stimulates ubiquitination of cell cycle proteins such as CDKs in addition to control the transition between G1/S and G2/M.

Roles in cytokinesis for NEKs have been widely proposed. For example, Nek6 and Nek7 may similarly regulate the localization of factors required for cytokinesis. In this respect, either NEK6 or NEK7 is localized at the midbody and depletion or expression of a kinase dead mutant protein together with mitotic spindle checkpoint inhibitors resulted in cytokinesis arrest for both kinases, [38]. In addition, NEK7 mouse knockout cells presented chromosome lagging, micronuclei formation, cytokinesis delay and aneuploidy [39]. In HeLa cells, genistein treatment, responsible for tubulin polymerization inhibition, also promotes DNA bridges and cytokinesis delay [40].

NEK3 has been described to be involved in neuronal morphology due to tubulin acetylation [20]. The suggested new role for NEK3 in DNA bridge formation and chromosomal instability may be also related to microtubule stabilization. Since chromosomal instability leads to mutations which result in tumor progression and also in cancer cell heterogeneity that drive multidrug resistance [41], the results shown in this work reinforce the roles for NEK3 in all stages of carcinogenesis.

4. Concluding Remarks

In this work, we performed a large scale screening for interaction partners of NEK3 by using the yeast two-hybrid system. We identified candidates interacting proteins that were functionally involved in SUMOylation, ubiquitinylation, transcriptional regulation, RNA processing, regulation of cell proliferation, invasiveness and metastasis. These processes are also involved with several steps of cancer progression and can be used to understand NEK3 function and behavior. NEK3 was found at the furrow of ingression and its depletion is associated to cytokinesis delay due to DNA bridges, that is related to aneuploidy, tetraploidy and micronuclei formation [37]. The role of NEK3 in DNA bridge formation may be related to microtubule stabilization, possibly via tubulin acetylation as observed for Nek3 signaling in neuronal cells [21].

In resume, this work has shown that NEK3 and its interaction partners are involved in multiple cancer stages through regulation of GTPase functions, among other signaling events. Different from other NEKs, NEK3 levels do not increase during cell cycle and its localization is not related to cilia function, but it is involved with DNA bridges formation and its knock down causes a cytokinesis delay. Also, this kinase localizes along with RhoA in the midbody, which has been previously described as essential for the cleavage furrow formation. Therefore, NEK3 may have novel important roles in the context of cytokinesis and the relevance of this new function in the context of cancer biology should be further explored.

5. Supplementary material

Supplementary data and information is available at http://www.jiomics.com/index.php/jio/rt/suppFiles/195/0

Supplementary Figure S1: NEK3 interactors in Yeast Two Hybrid Screening.

Supplementary Table S1: NEK3 interactome after Yeast two hybrid screen

Acknowledgments

The authors thank to Sao Paolo Research Foundation (FAPESP) (2010/51730-0, 2011/06730-5 and 2014/21700-3) and the Ministry of Science, Tecnology and Inovation / National Counsel of Technological and Scientific Development (MCTI/CNPq) for financial support through personal grant (471355/2012-0) and fellowships to VBC and JK. We also are grateful to Dr. Joan Roig (IRB-Barcelona) for his assistance in Nek3 shRNA oligo design and Nayara P. V. de Lira (LNBio) for figure design.

References

[1] S.L. Thompson, S.F. Bakhoum, D.A. Compton, Curr. Biol. 20 (2010) R285–R295. DOI: 10.1016/j.cub.2010.01.034

[2] K.P. Lu, B.E. Kemp, a R. Means, J. Biol. Chem. 269 (1994) 6603–6607.

[3] M.J. O'Connell, M.J.E. Krien, T. Hunter, Trends Cell Biol. 13 (2003) 221–228. DOI: 10.1016/S0962-8924(03)00056-4

[4] a M. Fry, E. a Nigg, Curr. Biol. 5 (1995) 1122–1125. DOI: 10.1016/S0960-9822(95)00227-2

[5] A.H. Osmani, K. O'Donnell, R.T. Pu, S.A. Osmani, EMBO J. 10 (1991) 2669–2679.

[6] B. Oakley, J. Cell Biol. 96 (1983) 1155–1158. DOI: 10.1083/jcb.96.4.1155

[7] S.A. Osmani, R.T. Pu, N.R. Morris, Cell 53 (1988) 237–244. DOI: 10.1016/0092-8674(88)90385-6

[8] A.M. Fry, Oncogene 21 (2002) 6184–94. DOI: 10.1038/sj.onc.1205711

[9] M. Govindaraghavan, A.A. Lad, S.A. Osmani, Eukaryot. Cell 13 (2014) 99–109. DOI: 10.1128/EC.00231-13

[10] G.V. Meirelles, A.M. Perez, E.E. de Souza, F.L. Basei, P.F. Papa, T.D. Melo Hanchuk, V.B. Cardoso, J. Kobarg, World J. Biol. Chem. 5 (2014) 141–60. DOI: 10.4331/wjbc.v5.i2.141

[11] M.R. Stratton, P.J. Campbell, P.A. Futreal, Nature 458 (2009) 719–724. DOI: 10.1038/nature07943

[12] C. Lengauer, K.W. Kinzler, B. Vogelstein, Nature 386 (1997) 623–7. DOI: 10.1038/386623a0

[13] C. Lengauer, K.W. Kinzler, B. Vogelstein, Nature 396 (1998) 643–9. DOI: 10.1038/25292

[14] P. Nowell, Science (80-.). 194 (1976) 23–28. DOI: 10.1126/science.959840
[15] Y. Chen, D.J. Riley, L. Zheng, P.L. Chen, W.H. Lee, J. Biol. Chem. 277 (2002) 49408–49416. DOI: 10.1074/jbc.M207069200
[16] D.G. Hayward, A.M. Fry, Cancer Lett. 237 (2006) 155–66. DOI: 10.1016/j.canlet.2005.06.017
[17] Y. Chen, P.-L. Chen, C.-F. Chen, X. Jiang, D.J. Riley, Cell Cycle 7 (2008) 3194–201. DOI: 10.4161/cc.7.20.6815
[18] S.L. Miller, J.E. Demaria, D.O. Freier, A.M. Riegel, C. V Clevenger, Mol Endocrinol. 19 (2005) 939–949. DOI: 10.1210/me.2004-0443
[19] S.L. Miller, G. Antico, P.N. Raghunath, J.E. Tomaszewski, C. V Clevenger, Oncogene 26 (2007) 4668–4678. DOI: 10.1038/sj.onc.1210264
[20] S.J. Schultz, a M. Fry, C. Sütterlin, T. Ried, E. a Nigg, Cell Growth Differ. 5 (1994) 625–635.
[21] J. Chang, R.H. Baloh, J. Milbrandt, J. Cell Sci. 122 (2009) 2274–82. DOI: 10.1242/jcs.048975
[22] D. Bar-Sagi, A. Hall, Cell 103 (2000) 227–238. DOI: 10.1016/S0092-8674(00)00115-X
[23] A.J. Ridley, Trends Cell Biol. 11 (2001) 471–477. DOI: 10.1016/S0962-8924(01)02153-5
[24] S. Aznar, P. Fernández-Valerón, C. Espina, J.C. Lacal, Cancer Lett. 206 (2004) 181–191. DOI: 10.1016/j.canlet.2003.08.035
[25] E. Sahai, C.J. Marshall, Nat. Rev. Cancer 2 (2002) 133–142. DOI: 10.1038/nrc725
[26] E.J. Park, K.-A. Ji, S.-B. Jeon, W.-H. Choi, I. Han, H.-J. You, J.-H. Kim, I. Jou, E.-H. Joe, J. Immunol. 173 (2004) 5697–5703. DOI: 10.4049/jimmunol.173.9.5697
[27] C.-T. Tsai, J.-L. Lin, L.-P. Lai, C.-S. Lin, S.K.S. Huang, Heart Rhythm 5 (2008) 1285–93. DOI: 10.1016/j.hrthm.2008.05.012
[28] C.J. Sherr, Science (80-.). 274 (1996) 1672–1677. DOI: 10.1126/science.274.5293.1672
[29] M.F. Carazzolle, L.M. de Carvalho, H.H. Slepicka, R.O. Vidal, G.A.G. Pereira, J. Kobarg, G.V. Meirelles, PLoS One 9 (2014) e100385. DOI: 10.1371/journal.pone.0100385
[30] P. Shannon, A. Markiel, O. Ozier, N.S. Baliga, J.T. Wang, D. Ramage, N. Amin, B. Schwikowski, T. Ideker, Genome Res. 13 (2003) 2498–504. DOI: 10.1101/gr.1239303
[31] A. Hershko, A. Ciechanover, Annu. Rev. Biochem. 67 (1998) 425–79. DOI: 10.1146/annurev.biochem.67.1.425
[32] M. Dasso, Cell Div. 3 (2008) 5. DOI: 10.1186/1747-1028-3-5
[33] Y.J. Jeon, K.Y. Lee, Y.-Y. Cho, A. Pugliese, H.G. Kim, C.-H. Jeong, A.M. Bode, Z. Dong, J. Biol. Chem. 285 (2010) 28126–33. DOI: 10.1074/jbc.M110.137190
[34] R.A. Reid, D.D. Bronson, K.M. Young, J.J. Hemperly, Mol. Brain Res. 21 (1994) 1–8. DOI: 10.1016/0169-328X(94)90372-7
[35] J.-M. Revest, C. Faivre-Sarrailh, N. Maeda, M. Noda, M. Schachner, G. Rougon, Eur. J. Neurosci. 11 (1999) 1134–1147. DOI: 10.1046/j.1460-9568.1999.00521.x
[36] J.-L. Su, P.-C. Yang, J.-Y. Shih, C.-Y. Yang, L.-H. Wei, C.-Y. Hsieh, C.-H. Chou, Y.-M. Jeng, M.-Y. Wang, K.-J. Chang, M.-C. Hung, M.-L. Kuo, Cancer Cell 9 (2006) 209–223. DOI: 10.1016/j.ccr.2006.02.018
[37] P. Morin, C. Flors, M.F. Olson, Eur. J. Cell Biol. 88 (2009) 495–507. DOI: 10.1016/j.ejcb.2009.04.005
[38] L. O'Regan, A.M. Fry, Mol. Cell. Biol. 29 (2009) 3975–90. DOI: 10.1128/MCB.01867-08
[39] H. Salem, I. Rachmin, N. Yissachar, S. Cohen, A. Amiel, R. Haffner, L. Lavi, B. Motro, Oncogene 29 (2010) 4046–4057. DOI: 10.1038/onc.2010.162
[40] Y. Nakayama, Y. Saito, S. Soeda, E. Iwamoto, S. Ogawa, N. Yamagishi, T. Kuga, N. Yamaguchi, J. Cell. Biochem. 115 (2014) 763–771. DOI: 10.1002/jcb.24720
[41] K.H. Allison, G.W. Sledge, Oncology (Williston Park). 28 (2014) 772–8.
[42] K. Mchale, J.E. Tomaszewski, R. Puthiyaveettil, V.A. Livolsi, C. V Clevenger, Mod. Pathology 21 (2008) 565–571. DOI: 10.1038/modpathol.2008.7

Special Issue
Selected Abstracts of the 5th International Congress on Analytical Proteomics (ICAP 2017)

The content published in this issue was previously selected by the scientific committee to be presented at the 5th International Congress on Analytical Proteomics, from 3 - 6 July 2017 in Caparica, Almada, Portugal. Only the Proceeding Abstracts with a copyright transfer agreement were reproduced.

Commitees

Conference Chairs

***Carlos Lodeiro Espiño*, PhD. FRSC**
UCIBIO-REQUIMTE, Chemistry Department, Universidade NOVA de Lisboa, Portugal.
***José Luis Capelo Martínez*, PhD. FRSC**
UCIBIO-REQUIMTE, Chemistry Department, Universidade NOVA de Lisboa, Portugal.

Scientific Committee

Carlos Lodeiro Espiño, PhD. FRSC
UCIBIO-REQUIMTE, Chemistry Department, Universidade NOVA de Lisboa, Portugal.
José Luis Capelo Martínez, PhD. FRSC
UCIBIO-REQUIMTE, Chemistry Department, Universidade NOVA de Lisboa, Portugal.
Christopher Overall, PhD
Centre of Blood Research, University of British Columbia, Canada.
William Laframboise, PhD
University of Pittsburgh School of Medicine, Pittsburgh, USA.
Francesc Canals, PhD
Laboratori de Protèomica, Institut d'Oncologia Vall d'Hebron (VHIO), Spain.
Juan J. Calvete, PhD
Instituto de Biomedicina de Valencia (CSIC)Instituto de Biomedicina de Valencia (CSIC) (Spain).
Gilberto Igrejas, PhD
Universidade de Trás-os-Montes e Alto Douro, Portugal.
Simona Francese, PhD
Sheffield Hallam University, Sheffield, United Kingdom.
Jens Coorssen, PhD
Brock University, Ontario, Canada.
Ola Söderberg, PhD
Department of Immunology, Genetics & Pathology, Uppsala University, Sweden.
Marco Zezzi Arruda, PhD
Universidade de Campinas, Campinas, Brasil.
Kay Ohlendieck, PhD
Maynooth University, Ireland.

Conference Secretariat

José Luis Capelo Martínez, PhD. FRSC
UCIBIO-REQUIMTE, Chemistry Department, Universidade NOVA de Lisboa, Portugal.
Marta Silva, MSc
UCIBIO-REQUIMTE, Chemistry Department, Universidade NOVA de Lisboa, Portugal.

JOURNAL OF INTEGRATED OMICS
A METHODOLOGICAL JOURNAL
HTTP://WWW.JIOMICS.COM

SPECIAL ISSUE: SELECTED ABSTRACTS OF THE 5TH INTERNATIONAL CONGRESS ON ANALYTICAL PROTEOMICS (ICAP 2017)

What can we learn from the proteomics of Arabidopsis plants grown in the International Space Station?

Christian Mazars [1*], Christian Brière [1], Sabine Grat [1], Carole Pichereaux [2], Michel Rossignol [2], Veronica Pereda-Loth [3], Brigitte Eche [3], Elodie Boucheron-Dubuisson [4], Isabel Le Disquet [4], Francisco Javier Medina [5], Annick Graziana [1], Eugénie Carnero-Diaz [4].

[1] Université de Toulouse UPS, CNRS UMR5546 Laboratoire de Recherches en Sciences Végétales, Castanet-Tolosan, France; [2] Plateforme Protéomique Génopole Toulouse Midi Pyrénées Institut de Pharmacologie et de Biologie Structurale IPBS CNRS-UMR5089 Toulouse France; [3] GSBMS, Université de Toulouse, France; [4] Université Pierre et Marie Curie – Paris 6, Sorbonne Universités, Institut de Systématique, Évolution, Biodiversité, ISYEB – UMR 7205 – CNRS, MNHN, UPMC, Paris, France; [5] Centro de Investigaciones Biologicas CSIC , Madrid, Spain.

Available Online: 5 June 2017

ABSTRACT

We present here the GENARA-A space experiment performed on board of the International Space Station (ISS) devoted to evaluate the qualitative and quantitative changes in membrane proteins supposed to be mainly associated with cell signaling in response to microgravity (µg) conditions. A selective and sequential extraction of proteins from microsomes prepared from seedlings grown on ISS, using salts, nonionic-detergent, chaotropic agents and ionic detergents provided us with various sets of protein extracts that were analyzed using LC MS/MS and quantified using a label-free method [1]. Among 1484 proteins quantified, 80 were significantly over-represented and 69 under-represented. Proteins linked to auxin metabolism and trafficking were depleted in membranes whereas proteins involved in stress responses, defense and metabolism were more abundant in µg conditions. Deeper analyzes of proteins whose abundance in membranes was not affected by microgravity but affected by 1g conditions between space and ground, indicated that large families of proteins were responsive to other parameters than gravity in space [2]. We discuss the possible consequences of such changes in abundance of proteins on the behavior of plants grown in space conditions. Increasing of such knowledge appears crucial in the future perspective to use plants as life support for long-term human spaceflights and space exploration.

Acknowledgments: The authors would like to thank NASA, the astronauts,the Norwegian User Support and Operations Center team (NUSOC) for its help in the preparation of the GENARA-A experiment and for their technical support during the carrying out of the experiment in the International Space Station. We acknowledge the European Aeronautic Defense and Space Company (Astrium EADS) for the design and building of the hardware and the European Space Agency (ESA) and the Centre National d'Etudes Spatiales (CNES) for their scientific and financial support.

References:

1] C. Mazars, C. Brière, S. Grat, C. Pichereaux, M. Rossignol, V. Pereda-Loth, B. Eche, E. Boucheron-Dubuisson, I. Le Disquet, F.J. Medina, A. Graziana, E. Carnero-Diaz; PLoS One. 9 (2014):e91814. doi: 10.1371/journal.pone.0091814

2] C. Mazars, C. Brière, S. Grat, C. Pichereaux, M. Rossignol, V. Pereda-Loth, B. Eche, E. Boucheron-Dubuisson, I. Le Disquet, F.J. Medina, A. Graziana, E. Carnero-Diaz; Plant Signal Behav. 9 (2014): e29637. doi: 10.4161/psb.29637

Correspondence: Email - mazars@lrsv.ups-tlse.fr

JOURNAL OF INTEGRATED OMICS
A METHODOLOGICAL JOURNAL
HTTP://WWW.JIOMICS.COM

SPECIAL ISSUE: SELECTED ABSTRACTS OF THE 5TH INTERNATIONAL CONGRESS ON ANALYTICAL PROTEOMICS (ICAP 2017)

Differences in the cardiac mitochondrial proteome between the right atria and right ventricle of congenital patients with ventricular septal defect

A.R. Bond [1*], M-S. Suleiman [1], S. Abdul-Ghani [1], D. Iacobazzi [1], K. Heesom [2], S.J. George [1], M. Caputo [1,3], R. Tulloh [1,3]

[1] Bristol CardioVascular, Research Floor Level 7, University of Bristol, Bristol, UK; [2] Proteomics Facility, University of Bristol, Bristol, UK; [3] Department of Congenital Heart Disease, King David Building, Bristol, UK

Available Online: 5 June 2017

ABSTRACT

Background: Despite known differences between the atria and the ventricles, researchers have been using atrial tissue to investigate ventricular cardiac molecular remodelling associated with congenital disease [1]. Ventricular septal defect (VSD), a hole in the septum between the left and right ventricle (RV) of the heart, is a common acyanotic congenital cardiac malformation that allows blood to pass from the left ventricle to the right ventricle of the heart. Due to the resulting increase in right ventricular pressure, pulmonary hypertension and RV hypertrophy develop. Mitochondrial remodelling occurs during ventricular hypertrophy. We hypothesise that disease induced remodelling in the hypertrophic ventricle is different to that of the atrium. Therefore, in this study we measured mitochondrial proteome in tissues collected from the right atrium (RA) and RV of patients with VSD to determine differences between these sites.

Methods: During open-heart surgery, biopsies of both the right atrium (RA) and right ventricle (RV) of age-matched infant VSD patients (n=5) were taken. Protein extracts were labelled with isobaric TMT reagents and underwent proteomic analysis. For phosphoproteomics analysis samples additionally underwent TiO_2 enrichment. A pooled sample was used as an internal control. Raw data files were processed and quantified using Proteome Discoverer v1.4 (Thermo Scientific) and searched against the UniProt Human database. All data were filtered to satisfy the FDR of 5%. Significant differences (paired t-test) between protein quantities (as a ratio of the pooled sample) of each chamber were determined and fold-changes ± 1.3 deemed of importance. Differences between individual phosphorylation sites of proteins were also compared. Analysis (PANTHER Database Version 11.1 [2]) of significantly changed proteins determined that mitochondrial proteins were overrepresented. Based on this outcome we focussed on the mitochondrial proteome by searching the dataset for the keyword 'mitochondria*' and using protein lists associated with the mitochondrial respiratory chain, derived from the HGNC database [3].

Results: Proteomic analysis yielded 3605 cardiac proteins of which 401 (11.1%) were mitochondrial. Of these, 30 (7.5%) were different between RA and RV; all being lower in the RA. These represented proteins involved in metabolic processes, assembly of respiratory chain complex IV, and mitochondrial translation, with the majority (30 proteins) having catalytic activity (Panther Overrepresentation Test). 414 phosphoproteins were identified in both chambers (represented by 700 individual phosphorylation site matches), however none were significantly altered.

Discussion: Despite being from the same patients, we have seen large differences in mitochondrial proteins from the different heart chambers. This may represent lower energy metabolism requirements due to the less contractile nature of the RA, or it may represent an overcompensation of the mitochondria in the RV due to increased pressure loading. There are clearly differences in the mitochondrial proteome between the RV and RA in patients with VSD. As such, caution should be used when drawing conclusions based on analysis of the RA and extrapolating to the hypertrophied RV in different pathologies.

Acknowledgments: We are grateful to SPARKS for funding this project, and the RVENCH Research Nurse team for coordinating patient consent and sample collection.

Correspondence: Email - andrew.bond@bristol.ac.uk

References

1] H. Zhang, D.X. Gong, Y.J. Zhang, S.J. Li, S. Hu; European Heart Journal 33 (2012) 1606-1614. doi: 10.1093/eurheartj/ehs061
2] H. Mi, Q. Dong, A. Muruganujan, P. Gaudet, S. Lewis, P.D. Thomas; Nucleic Acids Research 38 (2010) D204-D210. doi: 10.1093/nar/gkp1019
3] HGNC Database, HUGO Gene Nomenclature Committee (HGNC), European Bioinformatics Institute, www.genenames.org (accessed December 2016).

JOURNAL OF INTEGRATED OMICS
A METHODOLOGICAL JOURNAL
HTTP://WWW.JIOMICS.COM

SPECIAL ISSUE: SELECTED ABSTRACTS OF THE 5TH INTERNATIONAL CONGRESS ON ANALYTICAL PROTEOMICS (ICAP 2017)

Identification of new factors involved in PC12 neurite outgrowth regulated by dystrophins Dp71 and Dp40

Cecilia Montañez [1*], César García-Cruz [1], Candelaria Merino-Jiménez [1], Víctor Ceja [1], Jorge Aragón [1], Lourdes Siqueiros-Márquez [1], Juan Pablo Reyes-Grajeda [2]

[1] Departamento de Genética y Biología Molecular, Centro de Investigación y de Estudios Avanzados del IPN, Mexico City, Mexico, [2] Instituto Nacional de Medicina Genómica, Mexico City, Mexico.

Available Online: 5 June 2017

ABSTRACT

Dp71 and Dp40 are the shorter dystrophin isoforms of the Duchenne muscular dystrophy (DMD) gene. Dp71 protein is the most abundant product of this gene in the brain and the disruption of its expression has been related to the severity of the cognitive impairment observed in DMD patients [1]. The Dp71 gene generates several isoforms through alternative splicing, including dystrophin Dp40 which could play an important role in presynaptic function [2]. However, the specific function of each one of these dystrophins is unknown. With the aim of understanding the role of dystrophins Dp71 and Dp40, we partially characterized the proteome of PC12 cells overexpressing Dp71e, and mutants Dp71Δ78-79 and Dp40-L170P. We generated the mutant dystrophin Dp71Δ78-79 that lacks the two last exons because the C-terminal end corresponds to a region that differs between Dp71 isoforms. We reported that the Dp71Δ78-79 affects the expression of several proteins and stimulates neurite outgrowth mainly through upregulation and phosphorylation of HspB1 [3]. In this work, we evaluated the role of dystrophin Dp71e, an isoform expressed in PC12 cells, which lacks exons 78 and 79 and has 34 bp of intron 77. We found that the Dp71e overexpression stimulates the neurite outgrowth and promotes the upregulation of proteins involved in the differentiation process, in the cytoskeletal structuration as HspB1, S100A6 and K8, and in the neurotransmitter synthesis as HCNP as well as the neuronal marker TH. Additionally, we studied the dystrophin mutants Dp40-L170P and Dp40-ΔL170 (L3238, according to dystrophin Dp427). The deletion Δ3238 has been reported in patients with cognitive impairment [5]. Interestingly, both mutants Dp40-L170P [4] and Dp40-ΔL170 are predominantly distributed in the nucleus of transiently transfected PC12 cells. A morphometric analysis showed that the stably transfected PC12 Tet-On/Dp40-L170P cells are deficient in the neurite outgrowth compared to control PC12 cells. Through proteomic analysis of PC12 Tet-On/Dp40-L170P cells, we found that all proteins with differential expression were upregulated. One of these proteins was α-internexin, which is overexpressed when the axons are hindered to reach its target [6]. In summary, these results support the notion that the dystrophins Dp71e, Dp71Δ78-79 and Dp40 have a role in the regulation of proteins involved in the neurite outgrowth and this function is affected by the deletion of L170 in Dp40 (Dp40-ΔL170).

Correspondence: Email - cecim@cinvestav.mx

Figure 1| Cellular distribution of Dp71e and morphometric analysis in NGF-differentiated (9 days) PC12 Tet-On/Dp71e cells. (A) PC12 Tet-On/Dp71e and (B) control PC12 Tet-On (empty vector) cells observed by confocal microscope using anti-Myc monoclonal antibody (green). Nuclei were stained with DAPI (blue). The scale bar is equal to 25 μm. (C) Percentage of differentiation and (D) length of neurites in PC12 Tet-On/Dp71e cells compared to control PC12 Tet-On cells. ***P < 0.0001 denote statistical significance calculated using unpaired Student's t test.

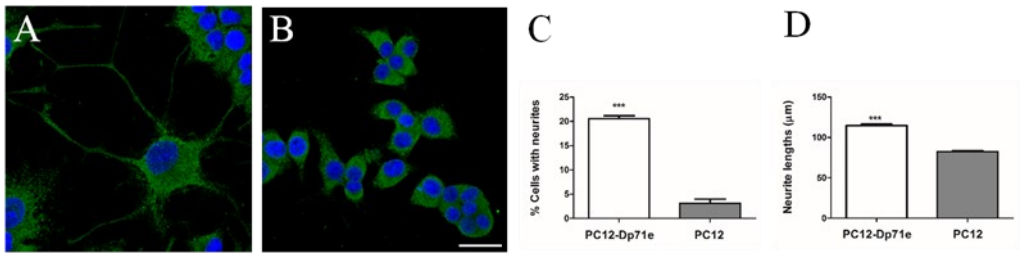

References

1] R. Tadayoni, A. Rendon, L. Soria-Jasso, B. Cisneros; Mol Neurobiol 45 (2012) 43–60.
2] T. Tozawa, K. Itoh, T. Yaoi, S. Tando, S. Fushiki; Mol Neurobiol 45 (2012) 287-297. doi: 10.1007/s12035-012-8233-5
3] C. Merino-Jiménez, J. Aragón, V. Ceja, C. Montañez; Proteomics 16 (2016) 1331-1340. doi: 10.1002/pmic.201500211
4] J. Aragón, A. Martínez-Herrera, C. Montañez; Neurosci Lett 600 (2015) 115-120. doi: 10.1016/j.neulet.2015.05.038
5] A.P. De Brouwer, W. Chen; Eur J Hum Genet 22 (2014) 480-485. doi:10.1038/ejhg.2013.169
6] T.S. McGraw, J.P. Mickle, G. Shaw, W.J. Streit; J Neurosci 22 (2002) 4955-4963.

JOURNAL OF INTEGRATED OMICS
A METHODOLOGICAL JOURNAL
HTTP://WWW.JIOMICS.COM

SPECIAL ISSUE: SELECTED ABSTRACTS OF THE 5TH INTERNATIONAL CONGRESS ON ANALYTICAL PROTEOMICS (ICAP 2017)

Quantitative dynamics of protein complexes in plant photosynthetic membranes upon light acclimation

Cristina Pagliano [1]*, Pascal Albanese [1], Marcello Manfredi [2], Emilio Marengo [3], Guido Saracco [4]

[1] Applied Science and Technology Department - BioSolar Lab, Politecnico di Torino, Viale T. Michel 5, 15121 Alessandria, Italy; [2] ISALIT - Department of Science and Technological Innovation, University of Eastern Piedmont, Viale T. Michel 11, 15121 Alessandria, Italy; [3] Department of Science and Technological Innovation, University of Eastern Piedmont, Viale T. Michel 11, 15121 Alessandria, Italy; [4] Center for Sustainable Future Technologies - CSFT@POLITO, Istituto Italiano di Tecnologia, Corso Trento 21, 10129 Torino, Italy

Available Online: 5 June 2017

Abstract

The thylakoid membrane is the site of the light-dependent reactions of photosynthesis. It harbors four main photosynthetic protein complexes: Photosystem I (PSI) and PSII, together with their antenna systems LHCI and LHCII, Cytochrome b6f and ATP-synthase. These complexes interact with supplementary proteins to ensure the metabolic flexibility required by plants to cope with ever-changing environmental conditions.

In this study, an extensive analysis of the Pisum sativum thylakoid membrane proteome was performed by thylakoid isolation from pea leaves, followed by protein extraction, in-solution trypsin digestion, mass spectrometry, and bioinformatics. A SWATH-MS (sequential window acquisition of all theoretical spectra-mass spectrometry) -based quantitative proteomic analysis [1] has been applied to investigate the thylakoid membrane proteome remodeling upon long-term acclimation of plants to low (LL), moderate (CL) and high (HL) light intensities. By exploiting transcriptomic data available for Pisum sativum, whose genome is only partially sequenced, a total 180 proteins were identified and quantified. Despite the evidence of a PSI/PSII ratio unaffected by long-term changes in light intensity, roughly half of the proteins was over-expressed in HL. Among them, there were several proteins involved in PSII disassembly and repair cycle, the ATP-synthase and the monomeric antenna Lhcb4.3. Conversely, the expression level of the major LHCII antenna proteins was reduced in HL.

In summary, SWATH analysis enabled a precise label-free comparative quantification on a thylakoid proteome scale. Taken together, our results demonstrate that the dynamics of the thylakoid membranes in plants grown at different light intensities is due to changes at the proteomic level, that ultimately determine the mechanisms by which plants can thrive in changing light conditions. These changes are a result of the fine-tuning of gene expression adopted by plants in response to long-term acclimation.

Acknowledgments: This work was supported by the Italian Ministry of Education, University and Research, "Futuro in Ricerca 2013" program RBFR1334SB to C.P.

References:

1] L.C. Gillet, P. Navarro, S. Tate, H. Röst, N. Selevsek, L. Reiter, R. Bonner, R. Aebersold; Mol. Cell. Proteomics 11 (6) :O111.016717 (2012). doi: 10.1074/mcp.O111.016717

Correspondence: Email - cristina.pagliano@polito.it

JOURNAL OF INTEGRATED OMICS
A METHODOLOGICAL JOURNAL
HTTP://WWW.JIOMICS.COM

SPECIAL ISSUE: SELECTED ABSTRACTS OF THE 5TH INTERNATIONAL CONGRESS ON ANALYTICAL PROTEOMICS (ICAP 2017)

Sarcomeric TPM3 expression in vertebrate hearts

Dipak K Dube [1]*, Syamalima Dube [1], Lynn Abbott [1], Kalpesh K. Shah [1], and Bernard J. Poiesz [1]

[1] Department of Medicine, SUNY Upstate Medical University, Syracuse, NY 13210, USA

Available Online: 5 June 2017

ABSTRACT

Tropomyosin is a component of thin filaments that constitute myofibrils, the contractile apparatus of striated muscles. In vertebrates, except for fish, four TPM genes *TPM1*, *TPM2*, *TPM3*, and *TPM4* are known. In zebrafish, there are six TPM genes that include the paralogs of the *TPM1* gene (*TPM1-1* & *TPM1-2*), the paralogs of the *TPM4* gene (*TPM4-1* & *TPM4-2*), and two single copy genes *TPM2* and *TPM3*. However, the functional significance of this diversity and how it may affect interactions with other sarcomeric proteins is not clear partly due to our incomplete knowledge of tropomyosin isoform diversity. To date, it is still not explicitly established whether *TPM3a* protein is expressed in human hearts. Interestingly, only one isoform of *TPM3* encoding a high molecular weight protein with 285 amino acid residues has been reported, which we call TPM3a. Recently, we have cloned and sequenced two more *TPM3* isoforms *TPM3v* and *TPM3ξ* both encode a protein with 285 amino acid residues. Of the two, one is termed *TPM3v* and the other is called *TPM3ξ* (Figure 1). *TPM3v* contains exon 6A in place of 6B and exon 9D in place of exon 9B as in *TPM3α*. Our other novel finding is the expression of *TPM3ξ* encoding identical protein like *TPM3α* but having a different 3'-UTR region – *TPM3ξ* contains 9D whereas *TPM3α* contains exon 9B . Our conventional RT-PCR data indicate that both isoforms are expressed in human heart and skeletal muscle and we are in the process of quantifying the expression level of these isoforms. As the expression of *TPM3α* protein in human heart is still disputed, we performed 2D Western blot analyses with human heart extract using CH1 monoclonal antibody that recognizes all sarcomeric isoforms with exon 9A. We detected 5 spots with positive signals. Next, each of the protein spots were analyzed by LC-MS/MS analyses. The amino acid sequences thus obtained show the presence of *TPM3ζ* in two spots. However, we failed to detect the sequence of exon 6A in either of the spots. Hence, we do not know whether *TPM3ξ* protein is expressed in human hearts. If it is expressed at such a low level that we are unable to detect this protein. In order to prove whether *TPM3a* is essential for cardiac contractility, one has to have a suitable animal model. However, using RNA PCR and 2D Western blotting and subsequent LC-MS/MS analyses we have established the expression of small quantities of *TPM3α* transcripts and protein in zebrafish hearts. We have not yet detected *TPM3v* in zebrafish. We have , however quantified the expression of *TPM3α* transcripts in zebrafish hearts. We believe we will be able to use zebrafish as an animal model to study whether *TPM3α* is involved in contractility in vertebrate hearts.

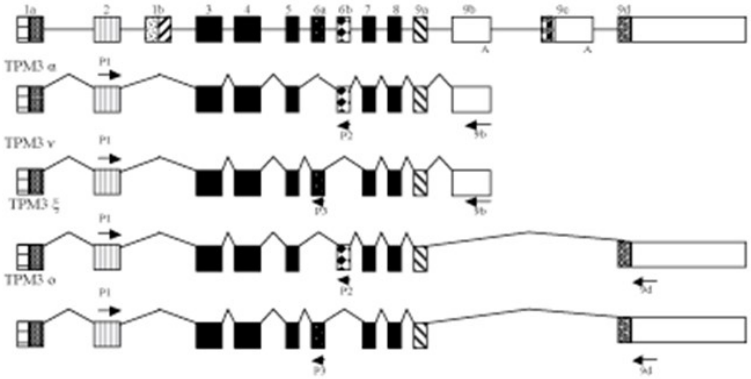

Figure 1. Three alternatively spliced isoforms *TPM3α*, *TPM3ν*, and *TPM3ξ* of the TPM3 gene. Primers P1& P2 for *TPM3ν* and *TPM3α* where as P1& P2 for *TPM3ξ* qRT-PCR. Oligo 9b and 9d will be used for making cDNA for *TPM3α* and TPM3ν respectively. Oligo 9d is for 9d.

Correspondence: Email - dubed@upstate.edu

JOURNAL OF INTEGRATED OMICS
A METHODOLOGICAL JOURNAL
HTTP://WWW.JIOMICS.COM

SPECIAL ISSUE: SELECTED ABSTRACTS OF THE 5TH INTERNATIONAL CONGRESS ON ANALYTICAL PROTEOMICS (ICAP 2017)

Salivary proteomics in ingestive behaviour research: advances, potentialities and limitations

Elsa Lamy [1*]

[1] ICAAM – Instituto de Ciências Agrárias e Ambientais Mediterrânicas, University of Evora, Portugal

Available Online: 5 June 2017

ABSTRACT

Human saliva proteomics gained interest in the last two decades, mostly due to the non-invasive nature of this fluid and its potential for the diagnosis of different oral and systemic pathologies. Curiously, despite saliva being the fluid that first contacts with food, only recently it has been an increased interest in the relationship between this fluid and ingestive behavior. The relevance of saliva protein composition in food acceptance and preferences is evidenced by the observation that individuals differing in oral food perception present particularities at level of salivary proteome. Individuals with different sensitivities for astringency diverge in the levels of several salivary proteins [1]. The same is true concerning the perception of basic tastes, namely bitter [2], [3] and sweet (Rodrigues et al., not published). Even aroma perception depends on saliva protein composition [4]. Interestingly, some of the proteins observed to differ in function of oral food perception are proteins that present variations with Body Mass Index (BMI) [5]. Besides this potential role of saliva in driving food choices, this fluid may have also potential as a source of biomarkers of ingestion. Although less explored, until now, there are evidences of changes in saliva protein composition based on the type of diet: diets rich in polyphenols induce modifications in saliva composition, in animal models [6], [7]; high-fat diets were also observed to change the levels of salivary alpha-amylase in rats [8]. It is interesting to note that the study of the link between salivary proteomics and ingestive behavior is useful in humans, but also in animal studies. Animal saliva has been less well explored, but it is gaining interest. However, there are some particularities that need to be considered, both at level of sample collection, treatment and protein identification [9]. These different points will be focused and critically discussed in the present presentation.

Acknowledgements: This study was funded by the FEDER as part of the Operational Programme for Competitiveness Factors – COMPETE and also received domestic funding from the FCT – Science and Technology Foundation – as part of Strategic Project PEst-OE/AGR/UI0115/2014 (ICAAM – University of Évora). Funding was additionally provided by the FCT – Portuguese Science Foundation: research contract IF/01778/2013 - Elsa Lamy.

References:

1] C. Dinnella, A. Recchia, S. Vincenzi, H. Tuorila, E. Monteleone; Chem. Senses 35 (2010) 75–85.
2] M. Dsamou, O. Palicki, C. Septier, C. Chabanet, G. Lucchi, P. Ducoroy, M.-C. Chagnon, M. Morzel; Chem. Senses 37 (2012) 87–95. doi: 10.1093/chemse/bjr070
3] T. Cabras, M. Melis, M. Castagnola, A. Padiglia, B. J. Tepper, I. Messana, I. Tomassini Barbarossa; PLoS One 7 (2012) p. e30962. doi: 10.1371/journal.pone.0030962
4] P. Piombino, A. Genovese, S. Esposito, L. Moio, P. P. Cutolo, A. Chambery, V. Severino, E. Moneta, D. P. Smith, S. M. Owens, J. A. Gilbert, D. Ercolini; PLoS One 9 (2014) p. e85611. doi: doi: 10.1371/journal.pone.0085611
5] E. Lamy, C. Simões, L. Rodrigues, A. R. Costa, R. Vitorino, F. Amado, C. Antunes, I. do Carmo; J. Physiol. Biochem. 71 (2015) 691–702. doi: 10.1007/s13105-015-0434-8
6] E. Lamy, G. Graça, G. da Costa, C. Franco, F. C. E Silva, E. S. Baptista, A. V. Coelho; Proteome Sci. 8 (2010) 65.
7] A. B. Beverly, L. Zhu, T. L. Fish, T. Thannhauser, M. A. Rutzke, D. D. Miller: J. Food Sci. 77 (2012).
8] L. Rodrigues, R. Mouta, A. R. Costa, A. Pereira, F. C. e Silva, F. Amado, C. M. Antunes, E. Lamy. Arch; Oral Biol. 60 (2015) 854-862.
9] E. Lamy & M. Mau; J. Proteomics 75(2012) 4251–4258.

Correspondence: Email - ecsl@uevora.pt

JOURNAL OF INTEGRATED OMICS
A METHODOLOGICAL JOURNAL
HTTP://WWW.JIOMICS.COM

SPECIAL ISSUE: SELECTED ABSTRACTS OF THE 5TH INTERNATIONAL CONGRESS ON ANALYTICAL PROTEOMICS (ICAP 2017)

Analysis of individual variation of *C. d. collilineatus* venom composition: implications in crotalic envenoming

Isadora Sousa de Oliveira[1*], Iara Aimê Cardoso[1], Karla de Castro Figueiredo Bordon[1], Sante Emmanuel Imai Carone[2], Johara Boldrini-França[1], Manuela Berto Pucca3, Karina Furlani Zoccal[2], José César Rosa4, Fabiani Gai Frantz[2], Lúcia Helena Faccioli[2], Suely Vilela Sampaio[2], Eliane Candiani Arantes[1]

[1] Department of Physics and Chemistry, School of Pharmaceutical Sciences of Ribeirão Preto, University of São Paulo, Ribeirão Preto, SP, Brazil; [2] Department of Clinical Analysis, Toxicology and Food Science, School of Pharmaceutical Sciences of Ribeirão Preto, University of São Paulo, Ribeirão Preto, SP, Brazil; [3] Health Sciences Center, School of Medicine, Federal University of Roraima, Boa Vista, RR, Brazil; [4] Protein Chemistry Center and Department of Molecular and Cell Biology and Pathogenic Bioagents, School of Medicine of Ribeirão Preto, University of São Paulo, Ribeirão Preto, SP, Brazil

Available Online: 5 June 2017

ABSTRACT

Crotalus durissus snakes are widely distributed in Brazilian territory[1,2] and show great variability in their venom composition, which can implicate in venom toxicity [3]. This feature may result in difficulties to select venoms to antivenom production [4,5,6,7]. Therefore, assessing these individual variations is necessary to understand the snakebite envenoming as well as to improve the antivenom production in order to obtain a more effective serum [5,8]. In this way, the aim of this study was to perform a comparative analysis of venom composition from 22 specimens of *C. d. collilineatus* using proteomics techniques following biochemical and immunological parameters evaluation in mice with the five venoms presenting the most variability in electrophoretical and chromatographic profiles. The venoms from 22 *C. d. collilineatus* snakes were fractionated on a RP-FPLC system using a C18 column [9] followed by SDS-PAGE [10] and mass spectrometry analysis. Although they have presented significant quantitative and qualitative differences in venom components, the chromatographic and electrophoretical profiles were similar. Nevertheless, it was possible to identify for the first time some components as NGF, ACE, phosphodiesterase, 5'-nucleotidase, carboxypeptidase, glutaminyl cyclase, glutathione peroxidase, NADH dehydrogenase and phospholipase B in *C. d. collilineatus* venoms by proteomic techniques. Furthermore, after the experimental crotalic envenoming in mice, it was observed that different venoms may lead to diverse biochemical and immunological effects, for example, the CK levels were different for each group of envenoming mice and only one of the venoms was able to induce significant production of NO. Thus, the victims of snakebite envenoming may present different clinical conditions. This study revealed unreported protein components *C. d. collilineatus* venom and demonstrated that differences in the venom composition of the same subspecies may lead to different pathophysiological effects during snakebite envenoming.

Acknowledgements: CAPES, FAPESP (2011/23236-4), CNPq and NAP-TOXAN-USP.

Correspondence: Email - **i**sadora_so@yahoo.com

References

1] J.A. Campbell & W.W. Lamar, *The venomous reptiles of Latin America.* 1989.
2] F.M.O. Pinho & I.D. Pereira*;* Rev Ass Med Brasil 47 (2001) 1: 24-29. doi: 10.1590/S0104-42302001000100026
3] L. da Silva Araújo, et al.; Revista Brasileira de Higiene e Sanidade Animal: RBHSA 10 (2016) 1 : 9-21. doi: 10.5935/1981-2965.20160002
4] G.T. Willemse*;* Comp Biochem Physiol (1978) 61B : 553-557.
5] J.-P. Chippaux, V. Williams, J. White; Toxicon 29 (1991) 11 : 1279-1303.
6] M.L. Ferreira, et al.; Toxicon 30 (1992) 12 : 1603-1608.
7] A.Jr. Lourenco, et al*.;* Toxicon 69 (2013) 75-81. doi: 10.1016/j.toxicon.2013.01.006
8] R.D.G. Theakston, D.A. Warrell, E. Griffiths; Toxicon 41 (2003) 5 : 541-557.
9] J.J. Calvete, P. Juarez, L. Sanz; J Mass Spectrom, 2007. 42 (2007) 11 : 1405-14. doi: 10.1002/jms.1242
10] U.K.Laemmli; Nature, 227 (1970) 680-685.

JOURNAL OF INTEGRATED OMICS
A METHODOLOGICAL JOURNAL
HTTP://WWW.JIOMICS.COM

SPECIAL ISSUE: SELECTED ABSTRACTS OF THE 5TH INTERNATIONAL CONGRESS ON ANALYTICAL PROTEOMICS (ICAP 2017)

Muscle, heart, brain and serum proteomics of X-linked muscular dystrophy

Kay Ohlendieck [1*], Sandra Murphy [1], Paul Dowling [1]

[1] Department of Biology, Maynooth University, National University of Ireland, Maynooth, Co. Kildare, Ireland

Available Online: 5 June 2017

ABSTRACT

Duchenne muscular dystrophy is the most frequently inherited neuromuscular disorder of early childhood and characterized by primary abnormalities in the *Dmd* gene, which causes the almost complete absence of the membrane cytoskeletal protein dystrophin of 427 kDa [1]. The full-length dystrophin isoform Dp427 forms a large protein complex in the plasma membrane of certain cell types in skeletal muscles, the heart and the central nervous system. Over the last few years, a large number of proteomic studies have investigated the dystrophin-glycoprotein complex and the secondary effects of the loss of dystrophin in X-linked muscular dystrophy [2]. Our laboratory has focused on the comparative proteomic profiling of the mdx and the mdx-4cv mouse models of dystrophinopathy with special emphasis on the elucidation of proteome-wide changes in various skeletal muscles, the heart, the brain and blood serum [3-6]. Proteomic findings from gel- and mass spectrometry-based investigations were verified by comparative immunoblotting surveys, enzyme-linked immunosorbent assays and immunofluorescence microscopy. New proteomic markers of (i) cellular degeneration and myofibrosis in dystrophic skeletal muscles, (ii) dystrophinopathy-associated cardiomyopathy, (iii) reactive gliosis in the dystrophin-deficient brain, and (iv) sterile inflammation in the serum were identified by mass spectrometry. These novel biomarker candidates can now be evaluated for their usefulness to improve diagnostic procedures, prognostic methods and therapeutic drug monitoring of X-linked muscular dystrophy.

Acknowledgements: Research was supported by project grants from the Deutsche Duchenne Stiftung *aktion benni & co e.V.*, the Health Research Board and Muscular Dystrophy Ireland, as well as a Hume scholarship from Maynooth University. The Q-Exactive quantitative mass spectrometer was funded under the Research Infrastructure Call 2012 by Science Foundation Ireland (SFI-12/RI/2346/3).

References

1] F. Rahimov, L.M. Kunkel; J. Cell Biol. 201 (2013) 499–510. doi: 10.1083/jcb.201212142
2] S. Murphy, K. Ohlendieck; Comput. Struct. Biotechnol. J. 14 (2015) 20-27. doi 10.1016/j.csbj.2015.11.002
3] S. Murphy, M. Zweyer, M. Henry, P. Meleady, R.R. Mundegar, D. Swandulla, K. Ohlendieck; Clin. Proteomics 12 (2015) 27. doi: 10.1186/s12014-015-9099-0
4] A. Holland, M. Henry, P. Meleady, C.K. Winkler, M. Krautwald, H. Brinkmeier, K. Ohlendieck; Molecules 20 (2015) 11317-11344. doi: 10.1016/j.csbj.2015.11.002
5] S. Murphy, P. Dowling, M. Zweyer, R.R. Mundegar, M. Henry, P. Meleady, D. Swandulla, K. Ohlendieck; J. Proteomics 145 (2016) 24-36. doi: 10.1016/j.jprot.2016.03.011
6] A. Holland, S. Murphy, P. Dowling, K. Ohlendieck; Proteomics 16 (2016) 345-366. doi: 10.1002/pmic.201500158

Correspondence: Email - kay.ohlendieck@nuim.ie

JOURNAL OF INTEGRATED OMICS
A METHODOLOGICAL JOURNAL
HTTP://WWW.JIOMICS.COM

SPECIAL ISSUE: SELECTED ABSTRACTS OF THE 5TH INTERNATIONAL CONGRESS ON ANALYTICAL PROTEOMICS (ICAP 2017)

Lipidation of viral proteins studied with MALDI-TOF MS

Larisa Kordyukova [1]*, Marina Serebryakova [1], Michael Veit [2]

[1]Belozersky Institute of Physico-Chemical Biology, Lomonosov Moscow State University, Russia; [2] Institut für Virologie, Free University Berlin, 14163 Berlin, Germany

Available Online: 5 June 2017

ABSTRACT

Enveloped viruses comprise a large number of dangerous pathogens entering the host cell via fusion of their lipid envelope with a target cellular membrane. The influenza virus hemagglutinin (HA) is a Class I prototypic glycoprotein responsible for this reaction. There is X-ray crystallography and cryoelectron microscopy data available for the HA ectodomain revealing its spiky architecture. In contrast, the HA anchoring segment is not resolved. This segment includes a transmembrane domain and a cytoplasmic tail that are post-translationally modified with long fatty acids. Using MALDI-TOF mass spectrometry, we studied differential S-acylation of influenza virus HA with palmitate and stearate. The isolation of hydrophobic peptides for the analysis involved either (1) enzyme proteolysis of purified virus particles followed by extraction with chloroform/methanol (ch/met) (Figure 1); (2) HA digestion within micelles of non-ionic detergent followed by ch/met extraction; or (3) HA electro-blotting to nitrocellulose membrane followed by in situ trypsin digestion, hexafluoroisopropanol (HFIP) and ch/met extraction. We have found site specific S-acylation of influenza virus HA: the location of the acylation site relative to the membrane border is the decisive factor for the attachment of stearate [1]. Various lipidated proteins might be analyzed with the developed approaches to get valuable structural information.

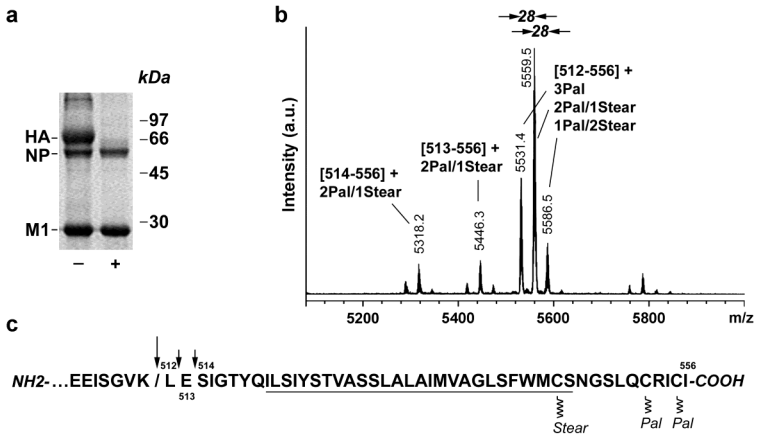

Figure 1| An example of MALDI-TOF-based analysis of fatty acylation: (a), SDS-PAGE analysis in non-reducing conditions of influenza virions before (-) or after (+) digestion with bromelain; (b), MALDI-TOF MS spectra with pointed average masses, the identified peptides and fatty acid patterns: three palmitates (3Pal), two palmitates and one stearate (2Pal/1Stear) or one palmitate and two stearates (1Pal/2Stear); (c), amino acid sequence of the HA C-terminus indicating sites of cleavage by bromelain (arrows). The transmembrane domain is underlined; the stearate and palmitate are schematically attached to the respective cysteine residues.

Acknowledgements: The work was supported by the Russian Foundation for Basic Research (grant 15-04-05044).

References

1] K. Brett, L.V. Kordyukova, M.V. Serebryakova, R.R. Mintaev, A.V. Alexeevski, M. Veit, J. Biol. Chem. 289 (2014) 34978-34989. doi: 10.1074/jbc.M114.586180

Correspondence: Email - kord@belozersky.msu.ru

JOURNAL OF INTEGRATED OMICS
A METHODOLOGICAL JOURNAL
HTTP://WWW.JIOMICS.COM

SPECIAL ISSUE: SELECTED ABSTRACTS OF THE 5TH INTERNATIONAL CONGRESS ON ANALYTICAL PROTEOMICS (ICAP 2017)

Calcium mobilisation in ventricles of paediatric patients with different malformations

M.-Saadeh Suleiman [1*], A Bond [1], M Caputo [1,2], S AbdulGhani [1], S George [1], S Stoica [2], M Wilson [3], K Heesom [3], R Tulloh [1,2]

[1]Bristol Heart Institute & School of Clinical Sciences, University of Bristol, Bristol, UK; [2] Paediatric Cardiac Services, Bristol Royal Hospital for Children, Bristol, UK ; [3] Proteomics Facility, Faculty of Biomedical Sciences, University of Bristol, UK

Available Online: 5 June 2017

ABSTRACT

Paediatric patients with congenital heart disease can be cyanotic or acyanotic depending on the malformation. Tetralogy of Fallot (TOF) and ventricular septal defect (VSD) are relatively two common pathologies that are associated with right ventricular hypertrophy. However, TOF can be chronically hypoxic and therefore considered as high risk during open heart surgery [1,2]. Understating cardiac molecular and cellular remodelling in these pathients provides important information that can help in the design of therapeutic interventions aimed at reducing reperfusion injury following cardioplegic arrest during open heart surgery. Loss of control over calcium (Ca^{2+}) mobilisation is key trigger of reperfusion injury. There are very few studies investigating pathology-induced changes in ventricular protein expression linked to Ca^{2+}-mobilisation. Therefore this study investigated the differences in the Ca^{2+} cycling proteins proteome and phosphproteome of TOF and VSD patients undergoing open heart surgery. Right ventricular tissues were collected from both pathologies. Patients (n=6/group) were matched for age. Protein extracts labelled with Tandem Mass Tag ten plex reagents (Thermo Fisher Scientific), were fractionated by high pH reversed-phase chromatography and analysed using nano-LC MSMS. Titanium dioxide (TiO2)-based phosphopeptide enrichment was used for phosphoproteomic analysis. Fold-change differences between protein values (ratio of pooled samples) were calculated and significance between groups was determined using unpaired t-test. Differentially expressed proteins (n=36) were detected. Six proteins were significantly higher in the TOF group which include adenylate cyclase, calcium/calmodulin-dependent protein kinase, phospholamban (PLN) & the ryanodine receptor. The following phosphoproteins were lower in TOF: PLN at S16, sarcoplasmic reticulum histidine-rich calcium-binding protein at S145 & Junctophilin-2 at T490. However, phosphorylated cardiac troponin I at S199 was higher in TOF. The finding for PLN-S16 is similar to other studies and was linked to effects of hypoxia and hypertrophy. The novel findings for the rest of the proteins/ phosphoproteins provide further evidence for maladaptation of the right ventricle in cyanotic TOF patients with implications for increased vulnerability to reperfusion injury during open heart surgery.

Acknowledgements: This study (Right VENtricle function in Children-RVENCH) is supported by the charity SPARKS. Ethical approval obtained for this work.

References

1] H. Imura, M. Caputo, A. Parry, A. Pawade, G. D. Angelini, M-S. Suleiman. Circulation 103 (2001)1551-1556. doi: 10.1161/01.CIR.103.11.1551

2] P. Modi, H. Imura, M. Caputo, A. Pawade, A. Parry, G. D. Angelini, M-S. Suleiman. J Thorac Cardiovasc Surg, 124 (2002)1035-1036.

Correspondence: Email - m.s.suleiman@bristol.ac.uk

JOURNAL OF INTEGRATED OMICS
A METHODOLOGICAL JOURNAL
HTTP://WWW.JIOMICS.COM

SPECIAL ISSUE: SELECTED ABSTRACTS OF THE 5TH INTERNATIONAL CONGRESS ON ANALYTICAL PROTEOMICS (ICAP 2017)

Working with antimicrobial plant peptides aiming biotechnological use

Maria Cristina Baracat-Pereira [1]*, Paulo Roberto Gomes Pereira [2], Tiago Antônio Oliveira Mendes [1], Alessandra Faria-Campos [3], Sérgio Vale Aguiar Campos [3]

[1]Department of Biochemistry and Molecular Biology & [2]Department of Plant Science, Universidade Federal de Viçosa, Viçosa, MG 36570-900, Brazil; [3] Department of Computer Science-ICEX, Universidade Federal de Minas Gerais, Av. Antônio Carlos 6627, Belo Horizonte, MG 31270-901, Brazil.

Available Online: 5 June 2017

ABSTRACT

Antimicrobial peptides from plants present mechanisms of action that are different from those of conventional defense agents. They are under-explored but have a potential as commercial antimicrobials. Bell pepper and egg-plant leaves are discarded after harvesting the fruit and are sources of bioactive peptides. This work reports the isolation by peptidomics tools and the partially characterization by computational tools of two antimicrobial peptides, one from bell pepper (*Capsicum annuum*) leaves, called HEV-CANN, and one from egg-plant (*Solanum melongena L.*) leaves, called CPI-SMEL, and evidences dificulties regarding the in silico analysis for the study of plant peptides. Mass spectrometry, automated peptide sequencing and bioinformatics tools were used alternately for identification and partial characterization of HEV-CANN, a Hevein-like peptide with 40 amino acid residues, 4258 Da, theoretical pI-value of 8.78, and four disulfide bonds, and for identification of CPI-SMEL, a Carboxypeptidase inhibitor peptide with 37 amino acid residues, 4089 Da, theoretical pI-value of 8.65 and three disulfide bonds. Computational tools used for proteomics and databases are not adjusted for short sequences, which hamper peptide identification. The adjustment of statistical tests in large databases for proteins is an alternative to promote the significant identification of peptides. The development of specific databases for plant antimicrobial peptides, with information about peptide sequences, functional genomic data, structural motifs and domains of molecules, functional domains, and peptide-biomolecule interactions are valuable and necessary.

Figure 1. Three-dimensional structures of the Hevein-like peptide from *Capsicum annuum* leaves (HEV-CANN, A) and the Carboxypeptidase inhibitor peptide from *Solanum melongena L.* Leaves (CPI-SMEL, B), both obtained by PHYRE²

Acknowledgements: The authors thank the Department of Plant Pathology (UFV), BIOAGRO (UFV), Núcleo de Análise de Biomoléculas (UFV), and LEM-CENARGEN (Embrapa, Brasília-DF, Brazil).

References

1] P.D. Games, E.Q.G. Silva, M.O. Barbosa, H.O. Almeida-Souza, P.P. Fontes, P.R.G. Pereira, M.V. Prates, G.R. Franco, A. Faria-Campos, S.V.A. Campos, M.C. Baracat-Pereira; BMC Genomics, 17 (Suppl 12) (2016) 1-13.

Correspondence: Email - baracat@ufv.br

JOURNAL OF INTEGRATED OMICS
A METHODOLOGICAL JOURNAL
HTTP://WWW.JIOMICS.COM

SPECIAL ISSUE: SELECTED ABSTRACTS OF THE 5TH INTERNATIONAL CONGRESS ON ANALYTICAL PROTEOMICS (ICAP 2017)

It's how you use it: Coomassie staining enables (sub)femtomole detection of intact gel-resolved proteoforms for Top-down Discovery Proteomics

Nour Noaman [1], Prabhodh S Abbineni [2], Michael Withers [1], Jens R Coorssen [3*]

[1]Department of Molecular Physiology, and the WSU Molecular Medicine Research Group, School of Medicine, Western Sydney University, Campbelltown, NSW, Australia ; [2] Department of Pharmacology, University of Michigan Medical School, Ann Arbor, Michigan, USA; [3] Faculty of Graduate Studies, and Departments of Health Sciences and Biological Sciences, Brock University, St Catharines, Ontario, Canada

Available Online: 5 June 2017

ABSTRACT

Two-dimensional gel electrophoresis (2DE) coupled with downstream "bottom-up" mass spectrometry (MS) continues to represent the most rigorous and practicable combination for an altogether routine Top-down approach to Proteomics. 2DE affords the highest available proteome resolution, offering sufficient resolving power to separate proteoforms in a single, reproducible assay[1]. Nonetheless, in-gel protein detection sensitivity (DS) must be rigorously addressed to ensure that gel-based methods provide optimal data for Discovery Proteomics. Experimental variables which impact DS must be controlled and optimized where possible to provide meaningful outcomes and further progression of this Top-down analytical approach[2].

Using protein standards independently assessed for purity, and resolved via modified 1DE models and 2DE – as well as 2DE of a native proteome – we demonstrate that the DS for intact 2DE-resolved proteins rivals that of MS for peptide detection, and is accomplished with common and cost-effective protein detection methods, i.e. an optimized colloidal Coomassie Brilliant Blue (cCBB) staining protocol coupled with near-infrared fluorescence detection [3-5], or densitometry. The data suggest that DS outcomes are highly dependent on image analysis software and associated methods for protein quantitation, and that image acquisition criteria are critical to enabling the most comprehensive mining of the resolved proteome. Optimizing imaging parameters and thus data input to provide the best possible analytical output enables more effective exploitation of the unprecedented and exceptional 2DE DS achievable with cCBB. Simply, the field now has access to high resolution, high sensitivity Top-down Proteomics that is both reasonably simple and cost effective.

Acknowledgements: NN and PSA received scholarship support from the WSU Molecular Medicine Research Group and the WSU School of Medicine, respectively. JRC notes the support of an anonymous private family foundation. NN is grateful to the Royal Society of Chemistry and the ProteoMass Scientific Society for receipt of a grant to attend V ICAP 2017.

References

1] J. Coorssen, A. Yergey; Proteomes, 3 (2015) 440-453. doi:10.3390/proteomes3040440
2] V.J. Gauci, N. Noaman, J.R. Coorssen; eLS, (2016). doi: 10.1002/9780470015902.a0002686.pub3
3] V.J. Gauci, M.P. Padula, J.R. Coorssen; Journal of Proteomics, 90 (2013) 96-106. doi: 10.1016/j.jprot.2013.01.027
4] R.H. Butt, J.R. Coorssen; Molecular & Cellular Proteomics, 12 (2013) 3834-50. doi: 10.1074/mcp.M112.021881
5] L.R. Harris, et al; J Proteome Res, 6 (2007) 1418-1425. doi: 10.1021/pr0700246

Correspondence: Email - jcoorssen@brocku.ca

JOURNAL OF INTEGRATED OMICS
A METHODOLOGICAL JOURNAL
HTTP://WWW.JIOMICS.COM

SPECIAL ISSUE: SELECTED ABSTRACTS OF THE 5TH INTERNATIONAL CONGRESS ON ANALYTICAL PROTEOMICS (ICAP 2017)

Amino acid content of alpha helices and beta strands depends on their flanking structures: development of a new ab-initio algorithm for secondary structure prediction

Khrustalev Vladislav Victorovich [1*], Khrustaleva Tatyana Aleksandrovna [2], Poboinev Victor Vitoldovich [1]

[1] Belarusian State Medical University, Minsk, Belarus; [2] Institute of Physiology of the National Academy of Sciences of Belarus, Minsk, Belarus

Available Online: 5 June 2017

ABSTRACT

There are two main factors that influence the formation of alpha helices and beta strands by polypeptide chains: intrinsic properties of amino acid residues and their combinations, and the influence of other parts of the same protein that are making contacts with a given fragment of a chain. In this study we showed that the last factor plays significant role, especially, in the formation of beta strands.

We used the set of 542 3D structures of bacterial proteins [1]. The proteins have been picked from proteomes of GC-poor and GC-rich bacteria, as well as from those with average genomic GC-content.

Amino acid usage in beta strands situated between two other beta strands is drastically different from the one in beta strands situated between two alpha helices. The usage of such hydrophilic amino acid residues, as Glu, Lys, Arg, Ser, Thr, Asn and Gln, as well as Tyr and Trp, are significantly higher in beta strands situated between two beta strands. The usage of the strongest beta strand forming amino acids (Val and Ile), as well as of Leu, Ala, Met and Cys are significantly higher in beta strands situated between two alpha helices. Beta strands situated between two alpha helices must be much more stable than those situated between beta strands. In the last case beta strands situated around can turn a hydrophilic sequence into another beta strand.

The differences between alpha helices situated between two other alpha helices and those situated between two beta strands are listed below: Lys, Asn, Gly and Cys are used significantly more frequently in alpha helices between beta strands, while Arg, Leu and Trp are used significantly more frequently in alpha helices between two other alpha helices. Alpha helices situated between alpha helix and beta strand also show some specific features relative to alpha helices situated between beta strand and alpha helix (Arg↑ ; Gln↑ ; Gly↓ ; Tyr↓), and relative to alpha helices situated between two alpha helices (Lys↑ ; Asn↑ ; Ala↓ ; Tyr↓ ; Trp↓).

We calculated the frequencies of combinations of two amino acids in all the types of alpha helices and beta strands and built propensity scales for the most stable beta strands (those situated between two alpha helices), and for the most stable alpha helices (those situated between two beta strands, and between alpha helix and beta strand). These scales together with the scale for the most stable coil (between two beta strands [1]) have been inserted into the PentaFOLD algorithm (http://chemres.bsmu.by). That algorithm has been used for the design of a prion peptide CC36 that contains a reconstructed part of a beta hairpin from a pathological form of prion protein [2].

References

1] V. V. Khrustalev, E. V. Barkovsky, T. A. Khrustaleva; International Journal of Proteomics 2014 (2014) 360230. doi: 10.1155/2014/360230
2] V. V. Khrustalev, T. A. Khrustaleva, K. Szpotkowski, V. V. Poboinev, K. Y. Kahanouskaya; Proteins 84 (2016) 1462 – 1479.

Correspondence: Email - vvkhrustalev@mail.ru

JOURNAL OF INTEGRATED OMICS
A METHODOLOGICAL JOURNAL
HTTP://WWW.JIOMICS.COM

SPECIAL ISSUE: SELECTED ABSTRACTS OF THE 5TH INTERNATIONAL CONGRESS ON ANALYTICAL PROTEOMICS (ICAP 2017)

Biphasic changes in survival signalling protein expression during postnatal development; the association with vulnerability to ischemia-reperfusion injury

Kim Summers [1], Martin Lewis [1], Hua Lin [1], Kate Heesom [2], Massimo Caputo [1], M.-Saadeh Suleiman [1]

[1]School of Clinical Sciences, University of Bristol, UK; [2] School of Biochemistry, University of Bristol, UK

Available Online: 5 June 2017

ABSTRACT

Rationale: It has previously been demonstrated that cardiac recovery following ischemia-reperfusion injury displays a biphasic pattern of change over the course of postnatal development, with the greatest degree of functional recovery seen in rats of approximately 14 days of age (Figure 1A1). The underlying cause for these differences in vulnerability to cardiac insult are currently unknown, and the majority of mechanisms proposed do not account for the precise biphasic pattern of change seen. Due to the importance of pathways such as Reperfusion Injury Salvage Kinase (RISK) & Survivor Activating Factor Enhancement (SAFE) in promoting cell survival following cardiac insult, as well as in current methods of cardioprotection, we hypothesise that it is differences in such signalling pathways and their constituent proteins at different stages of postnatal development that account for these biphasic changes in cardiac recovery.

Methods: Three runs of Tandem Mass Tag 10-plex (TMT10plex) analysis were performed on cardiac extracts from 7 day (n=4), 14 day (n=8), 28 day (n=8) and adult (n=7) rats, each sample labelled with a unique reporter group (126 N/C, 127 N/C, 128 N/C, 129 N/C, 130 N/C), before pooling into a single sample (131). Following LC-MS/MS analysis, proteins involved in survival signalling pathways were identified within the resulting proteomic output, and analysed for statistically significant changes using Oneway-ANOVA.

Results: Over 300 proteins linked to key survival signalling pathways, either as direct effectors or as upstream or downstream targets, were found to display statistically significant biphasic changes in expression, peaking or dropping at 14 days of age. Of particular interest, crucial components of the RISK and SAFE signalling pathways such as Akt1, ERK1, JAK1 and STAT3, as well as downstream targets such as PKCε, showed the greatest expression in 14 day old hearts.

Conclusion: Our data indicate a strong correlation between the expression of survival signalling related proteins and the biphasic changes in cardiac vulnerability to ischemia-reperfusion injury seen in rat hearts. Whilst further investigation will be required to determine a causal role further to this currently associative relationship, our findings provide support for the mechanistic role of survival signalling pathways in the improved recovery following injury seen in 14 day old rats, and highlight potential proteins of interest for future therapeutic strategies in the treatment of this form of cardiac insult.

References

1] Modi, P. and M.-S. Suleiman. Amino acids 26 (2003) 1 : 65-70. doi: 10.1007/s00726-003-0031-y

Correspondence: Email - vvkhrustalev@mail.ru

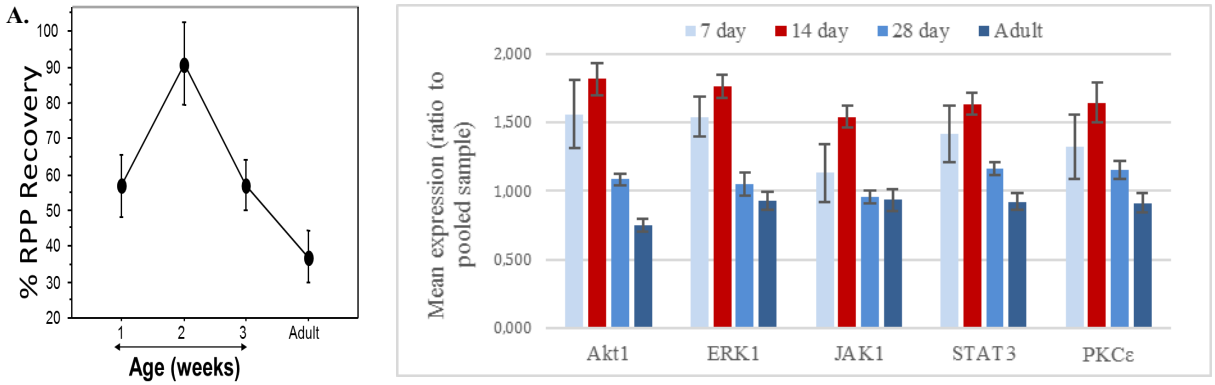

Figure 1| A. The biphasic change in functional recovery following Ischemia-Reperfusion injury during postnatal development in rats (RPP = Rate-Pressure Product).[1] **B.** Examples of biphasic changes in the expression of key survival signalling-related proteins.

JOURNAL OF INTEGRATED OMICS
A METHODOLOGICAL JOURNAL
HTTP://WWW.JIOMICS.COM

SPECIAL ISSUE: SELECTED ABSTRACTS OF THE 5TH INTERNATIONAL CONGRESS ON ANALYTICAL PROTEOMICS (ICAP 2017)

Proteomic and Interactome approaches reveal new targets of the Cdc42 GTPase in cellular conditions of genomic instability

Renan C. Souza [1], Eduardo S. Kitano [2], Leo K Iwai [2], and Fabio L. Forti [1]*

[1] Laboratory of Signaling in Biomolecular Systems (LSBS), Department of Biochemistry, Institute of Chemistry, University of Sao Paulo, Sao Paulo, Brazil. [2] Laboratório Especial de Toxinologia Aplicada (LETA), Center of Toxins, Immune-Response and Cell Signaling (CeTICS), Instituto Butantan, Sao Paulo, Brazil.

Available Online: 5 June 2017

ABSTRACT

The Cdc42 proteins (Cell Division Cycle 42), a member of the Rho family of GTPases, are intracellular signaling molecules well known for their role in the cytoskeleton regulation [1]. This protein cycles between an active state (GTP-bound) and an inactive state (GDP-bound) and this regulation is modulated by proteins known as GEFs, GAPs and GDIs. Recent studies demonstrated roles for Cdc42 in apoptosis and senescence, cellular responses commonly triggered by genotoxic stress [2]. More specifically, in some tumor cells the Cdc42 constitutively active mutant, Cdc42-V12, was shown to act as anti-proliferative GTPase [3]. This work sought to identify Cdc42 interactions with other proteins possibly involved in DNA damage response and repair mechanisms. To reach these aims we used HeLa and MRC-5 cell lines submitted to treatments with ultraviolet C radiation to induce DNA damage. Two experimental conditions were used for each cell line, with different times and doses post UV irradiation, in order to search for proteins involved in either rapid or delayed response to the installed DNA damage. Cell lysates obtained from these treatments were subjected to pull-down experiments using recombinant proteins GST, GST-Cdc42-WT (Wild type) and GST-Cdc42-V12. Purified proteins were digested by trypsin, analyzed by mass spectrometry and the obtained data were used for the construction of protein-protein interaction (PPI) networks. Among the identified proteins those seemingly more relevant to the aims of this work are: Prohibitin-2 (PHB2), found in samples incubated 48 hours post irradiation; Cullin-4A (CUL4A) and P53, found in samples incubated 5 minutes after radiation. These proteins have roles in apoptosis and DNA repair and were observed in close proximity to Cdc42 in PPI networks, in addition to other proteins belonging to canonical DNA repair mechanisms, making them interesting targets for future validation by different experimental approaches. These findings are in accordance with biological assays showing that cells over activating Cdc42 are more sensitive to DNA effects of UV radiation.

Acknowledgements: We thank to Prof. Solange M.T. Serrano and to the technician Ismael F. Lima for the reagents and use of the mass spectrometry facility. We also thank to the Brazilian funding agencies Fapesp, CNPq and Capes for supporting this research.

References:

1] Cerione RA. Trends Cell Biol; 14 (2004) 3 127-132. doi: 10.1016/j.tcb.2004.01.008
2] Wang L, Yang L, Debidda M, Witte D, Zheng Y. Proc Natl Acad Sci USA: 104 (2007) 4 1248-1253. doi: 10.1073/pnas.0609149104
3] Ascer LG, Magalhaes YT, Espinha G, Osaki JH, Souza RC, Forti FL. J Cell Biochem. 116 (2015) 9 2086-97. doi: 10.1002/jcb.25166

Correspondence: Email - flforti@iq.usp.br

JOURNAL OF INTEGRATED OMICS
A METHODOLOGICAL JOURNAL
HTTP://WWW.JIOMICS.COM

SPECIAL ISSUE: SELECTED ABSTRACTS OF THE 5TH INTERNATIONAL CONGRESS ON ANALYTICAL PROTEOMICS (ICAP 2017)

Reproducibility in gel-based protein and proteome analysis: External and internal standardisation with Comparative 2D Fluorescence Gel Electrophoresis CoFGE

Simone König [1]

[1] IZKF Core Unit Proteomics, University of Münster, Germany

Available Online: 5 June 2017

ABSTRACT

A major problem for the acceptance of two-dimensional (2D) protein gel electrophoresis for proteome analysis has been the lack of comparability of gel images among different laboratories or even within the same working group. Now, the generation of a reference grid of marker proteins in parallel to the separation of the analyte allows the correction of protein coordinates both in x (protein isoelectric point)- and y (molecular weight)-direction. This is achieved by use of multiple fluorescent dyes for standards and samples on the same gel. A net of ~100 marker nodes spans the gel and provides reference points for triangulation (Figure 1). The deviation from mean is improved by an order of magnitude. The technology termed Comparative 2D Fluorescence Gel Electrophoresis (CoFGE) can be carried out in both vertical and horizontal electrophoresis instrumentation with the latter being much more comfortable. With CoFGE, archiving of coordinates of proteins identified by mass spectrometry in databases has become reality and a Repository of Gel-Separated Proteins (ReGeSeP) was generated for storing and searching protein IDs, coordinates and proteome gel images. The technology was licensed and awarded with the WWU Transfer Prize 2013/2014. [1-4]

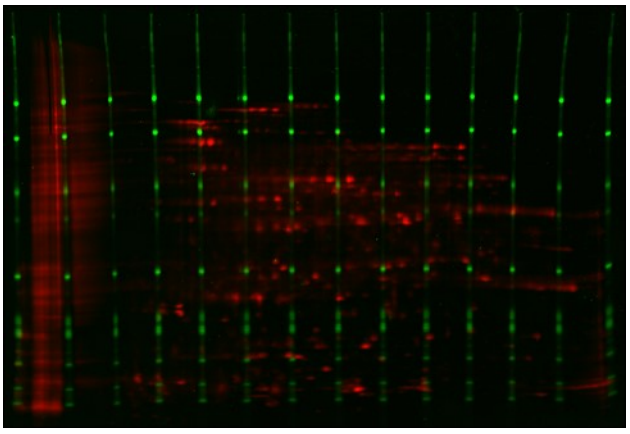

Figure 1| False-color image of a horizontal CoFGE experiment (*E. coli* - red, marker grid - green).

Correspondence: Email - koenigs@uni-muenster.de

References

1] D. Ackermann, S. König, Comparative 2D fluorescence gel electrophoresis. In: Difference gel electrophoresis – Methods and protocols. In: Methods in Molecular Biology, Springer 2017

2] M. Hanneken, K. Slais, S. König,; EuPa Open Proteomics 8 (2015) 36-39. Data in Brief 3: 221-228. doi: 10.1016/j.dib.2015.03.007

3] M. Hanneken, S. König; Electrophoresis 35 (2014) 1118-1121. doi: 10.1002/elps.201300507

4] D. Ackermann, W. Wang, B. Streipert, B. Geib, L. Grün, S. König; Electrophoresis 33 (2012) 1406-1410. doi: 10.1002/elps.201200039. D. Ackermann, W. Wang, L. Grün, S. König, Patent application EP11167383.6, May 25, 2011.

JOURNAL OF INTEGRATED OMICS
A METHODOLOGICAL JOURNAL
HTTP://WWW.JIOMICS.COM

SPECIAL ISSUE: SELECTED ABSTRACTS OF THE 5TH INTERNATIONAL CONGRESS ON ANALYTICAL PROTEOMICS (ICAP 2017)

Combined omics techniques in Nanotoxicology

Sabrina Gioria [1*], Joana Lobo Vicente [1], Paola Barboro [2], Rita La Spina [1], Giorgio Tomasi [3], Patricia Urbán [1], Agnieszka Kinsner-Ovaskainen [1], François Rossi1, Hubert Chassaigne1

[1] European Commission, Joint Research Centre (JRC), Directorate for Health, Consumers and Reference Materials, Consumer Products Safety Unit, Via Enrico Fermi 2749, I-21027 Ispra (VA), Italy; [2] Academic Unit of Medical Oncology, Ospedale Policlinico San Martino, L.go R. Benzi 10, 16132, Genova, Italy; [3] University of Copenhagen, Nørregade 10, DK-1017 Copenhagen, Denmark

Available Online: 5 June 2017

ABSTRACT

Omics technologies, such as proteomics or metabolomics, have to date been applied in the field of nanomaterial safety assessment to a limited extent. To address this dearth, we developed an integrated approach combining the two techniques to study the effects of two sizes, 5 and 30 nm, of gold nanoparticles (AuNPs) in Caco-2 cells. We observed differences in cells exposed for 72 h to each size of AuNPs: 61 responsive (up/down-regulated) proteins were identified and 35 metabolites in the cell extract tentatively annotated. Several altered biological pathways were highlighted by integrating the obtained multi-omics data with bioinformatic tools. This provided a unique set of molecular information on the effects of nanomaterials at cellular level. This information was supported by complementary data obtained by immunochemistry, microscopic analysis and multiplexed assays. A part from increasing our knowledge on how the cellular processes and pathways are affected by nanomaterials (NMs), these findings could be used to identify specific biomarkers of toxicity or to support the safe-by-design concept in the development of new nanomedicines [1].

References

1] S. Gioria, J. Lobo Vicente, P. Barboro, R. La Spina, G. Tomasi, P. Urbán, A. Kinsner-Ovaskainen, R. François, H. Chassaigne; Nanotoxicology 10 (2016) 6 : 736-48. doi: 10.3109/17435390.2015.1121412

Correspondence: Email - sabrina.gioria@ec.europa.eu

JOURNAL OF INTEGRATED OMICS
A METHODOLOGICAL JOURNAL
HTTP://WWW.JIOMICS.COM

SPECIAL ISSUE: SELECTED ABSTRACTS OF THE 5TH INTERNATIONAL CONGRESS ON ANALYTICAL PROTEOMICS (ICAP 2017)

Reproductive Isolation in Marine Mussels (*Mytilus* spp.)

Angel P. Diz [1,2*]

[1]Department of Biochemistry, Genetics and Immunology, University of Vigo, Vigo, Spain; [2]Toralla Marine Science Station (ECIMAT), University of Vigo, Isla de Toralla, Vigo, Spain.

Available Online: 5 June 2017

ABSTRACT

The study of the mechanisms that lead to the formation of new species is of special interest in marine ecosystems due to the lack of obvious barriers to gene flow. Mussels of the genus *Mytilus* are marine organisms with external fertilization able to hybridize where the distribution of two species overlap, allowing the study of reproductive isolation mechanisms in a natural scenario. Because the formation of hybrids is so frequent between *Mytilus* spp., it is likely that different types of reproductive barriers, both at pre- and post-zygotic levels, might be playing a role to preserve the genome integrity of each species. The relative contribution and underlying molecular mechanisms of each are far from clear. Choosing reproductive tissue or gametes as the main research target should help to elucidate some of these basic aspects in reproductive and evolutionary biology. An integrated approach combining results from different -omic levels represents the preferred strategy in order to reach more realistic conclusions. I will present results from ongoing research in my lab with different populations of two *Mytilus* spp., including mussels from a hybrid zone. Results will be discussed from an evolutionary ecology viewpoint.

Acknowledgments: Research work was funded by Ministerio de Economía y Competitividad (projects codes BFU2011-22599 and AGL2014-52062-R), Fondos FEDER and Xunta de Galicia ("Grupos de Referencia Competitiva", ED431C 2016-037).

Correspondence: Email - angel.p.diz@uvigo.es

JOURNAL OF INTEGRATED OMICS
A METHODOLOGICAL JOURNAL
HTTP://WWW.JIOMICS.COM

SPECIAL ISSUE: SELECTED ABSTRACTS OF THE 5TH INTERNATIONAL CONGRESS ON ANALYTICAL PROTEOMICS (ICAP 2017)

Comprehensive metaboproteomic analysis of different lymphoma

Philipp Schwarzfischer [1], Jörg Reinders [1], Katja Dettmer [1], Karsten Kleo [2], Lora Dimitrova [2], Michael Hummel [2], Maren Feist [3], Dieter Kube [3], Monika Szczepanowski [4], Wolfram Klapper [4], Franziska Taruttis [5], Julia C. Engelmann [5], Rainer Spang [5], Wolfram Gronwald [1], Peter J. Oefner [1*]

[1] Institute of Functional Genomics, University of Regensburg, Germany, [2] Institute of Pathology, Charité-University Medicine Berlin, Germany; [3] Department of Hematology and Oncology, University Medical Center Goettingen, Germany; [4] Institute of Hematopathology, University Hospital Schleswig-Holstein, Kiel, Germany; [5] Chair of Statistical Bioinformatics, University of Regensburg, Germany

Available Online: 5 June 2017

ABSTRACT

Burkitt's lymphoma (BL) and diffuse large B-cell lymphoma (DLBCL) are pathologically and clinically distinct subtypes of aggressive non-Hodgkin B-cell lymphoma. A comprehensive metaboproteomic approach was conducted to study both established cell lines as well as cryopreserved tissue sections. Therefore, NMR- and MS-based metabolome analyses were complemented by SWATH-MS-based quantitative proteomics. Furthermore, the proteomic approach was also extended to formalin-fixed paraffin-embedded (FFPE) tissue sections of BL and DLBCL. Thereby, a comprehensive analysis on both metabolomics and proteomic level was accomplished which allows deeper insight into tumour- and tumour-environment-based processes. Moreover, we were able to show comparability and relevance of cell culture findings in different tissue specimens as well as transferability of marker proteins from the SWATH-analyses to further techniques like immunohistochemistry.

Correspondence: Email - joerg.reinders@ukr.de